PACMAN FLOWPAD^3
COTS DIFFERENTIAL LNAs

Roberto García García

INFORME TÉCNICO IT-OAN 2008-1

PACMAN FLOWPAD^3
COTS DIFFERENTIAL LNAs

Roberto García García
FG-IGN (Spain)

CONTENTS

LIST OF FIGURES

LIST OF TABLES

1.- INTRODUCTION

This report shows the work done by the author during three months of trainee-ship at ASTRON (Netherlands Foundation for Research in Astronomy). An evaluation of different COTS DLNA (Differential Low Noise Amplifiers) was carried out in order to check if there are any commercial differential amplifiers that potentially fulfil the noise specifications for the mid-band range of the SKA telescope (300MHz- 1GHz) [1].

Specifically, this work is part of the demonstrator FLOWPAD^3 (funded by ASTRON). FLOWPAD^3 is a demonstrator used to show innovative technologies which were studied during the PACMAN and SKADS DS4T4 projects. It consists of an active phased array tile of differential tapered slot active antenna elements.

Three demonstrators will be built with all of them using the same mechanical structure and the same antenna [2], but with different LNA chips. The first demonstrator will have a commercial LNA, while the second and the third will be built with custom LNAs designed at ASTRON.

The main target of PACMAN project is to reduce the cost as much as possible. The strategy is to use Vivaldi antennas printed over a very thin foil of Polyester or Kapton. These antennas will be placed into a foam structure of Polypropylene in order to keep the foils straight and give to the array the desired lattice (as is shown in Fig. 1).

Figure 1: Foam structure for an array tile and polyester antenna elements.

1.1.-SPECIFICATIONS

The specifications for the FLOWPAD^3 demonstrator are shown [2] in the following table:

Antenna element	Vivaldi with differential feeding	• Not been made before • Potentially cheaper • Potentially less noisy than single ended (less losses in antenna feed network).
Polarization	Dual polarization	Memo45 requirement
Frequency band	300-1000 MHz	SKADS bench mark design
Antenna pitch	176 mm (=½ λ @ 850 MHz)	Modified SKADS bench mark design (from 800 to 850). Enables max 1000 MHz freq.
Tile size	8x8 = 64 elements (32 per polarization)	Related to beam forming. 4:1
Beam former	Optional; no steering	Demonstrated by EMBRACE
Tsys	35 K	System = antenna + LNA
Gain	COTS LNA: 20 dB Custom 1 LNA: 20-30 dB Custom 2 LNA: reduced slope	
Antenna Impedance	150 Ω	
Output of the active antenna element	Single	Output balun included in LNA board
Supply	Via RF coaxial	Cost / crosstalk/ oscillation

Table 1: System Specifications

FLOWPAD^3 is the first SKADS demonstrator that uses a fully differential Vivaldi antenna. It is expected that a differential configuration yields a smaller noise temperature because of the lossy balun is removed of the feeding network.

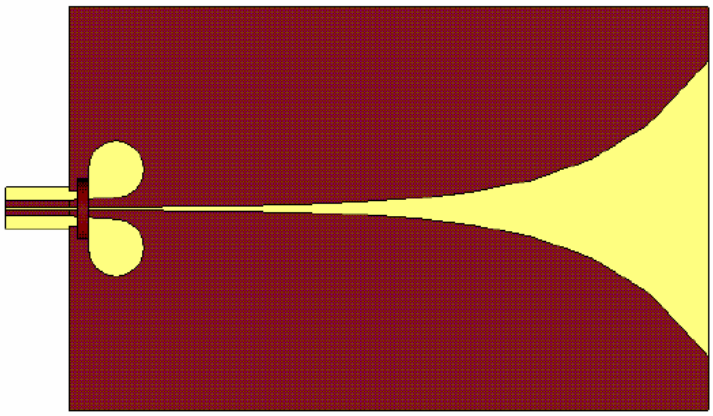

Figure 2: Differential Vivaldi antenna.

Instead of using a microstrip feed line (previous prototypes), the feeding line is a differential line (Coplanar Strips Line, -.CPS.-). a connection is needed between the side planes of the Vivaldi antenna, through a bridge or an equivalent structure, in order to avoid unexpected results.

Some of the parameters of the antenna element (dimensions, bridges, cavities, etc.) were analyzed in [2]. For example the size of the cavity has a direct effect on the frequency band of the feeding system. On the other hand, the shape of the cavity has an effect on the final performance of the system.

Figure 3 shows the connection between the antenna and the DLNA PCB. It consists on swapping the original metallic bridge with a connection using a strip line on the DLNA board. The effect of this connection was simulated in [2] using a RO4003 substrate (ε_r = 3.38 and t = 0.8 mm) as a PCB. The results of replacing the original metallic bridge with the DLNA PCB are found to be similar.

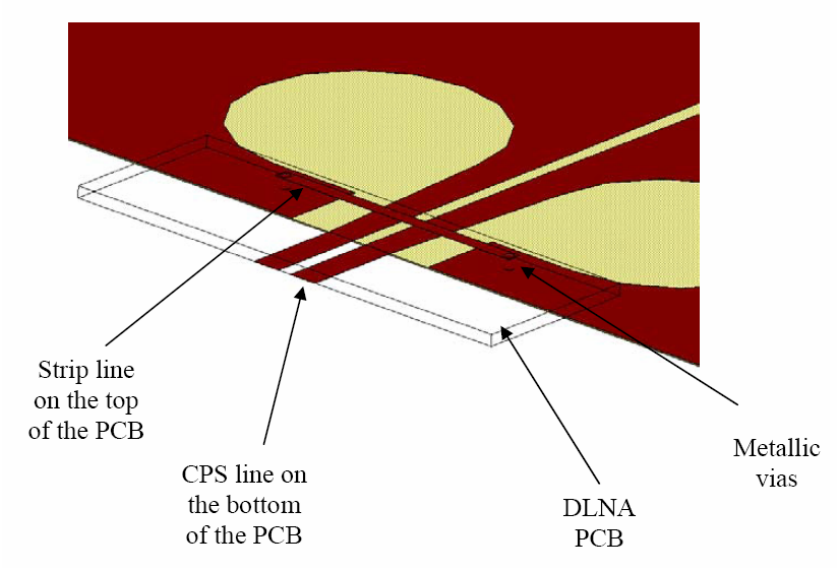

Figure 3: Differential Vivaldi antenna.

1.2.- ADVANTAGES AND DISADVANTAGES OF A DLNA

Balanced differential circuits have been used for a number of years in low-frequency applications in order to provide high-noise immunity and to eliminate the ground connection as the signal-return path. In general, there are three advantages to differential circuits as compared to single-ended circuit implementations, which are accelerating their use in RF and microwave systems [3]:

- Improved noise isolation
- Increased dynamic range for a given supply voltage
- Reduced even-order distortion.

Nevertheless, there are some disadvantages that have slowed down the use of differential circuits instead of single-ended ones:

- Double the circuitry versus a single-ended design
- Twice the current and power consumption

- Difficult to design and analyze (differential and common propagation modes)
- Not easily characterized (the standard measurement equipment can not be used)

In the specific application that is been described, the main advantage of using a DLNA is that does not require a balanced to unbalanced (BALUN) transition. As the antenna element is differential, the LNA can be connected directly to the Vivaldi terminals. The balun transition is lossy, noisy, frequency dependant and additional board layers could be needed. However, the DLNAs are not common in radio-astronomy yet.

The extension of standard two-port s-parameters to four-port differential circuits and the presence of new four-port test equipment should minimize the last two disadvantages [3]. However, equipment for noise figure measurements has not been developed yet.

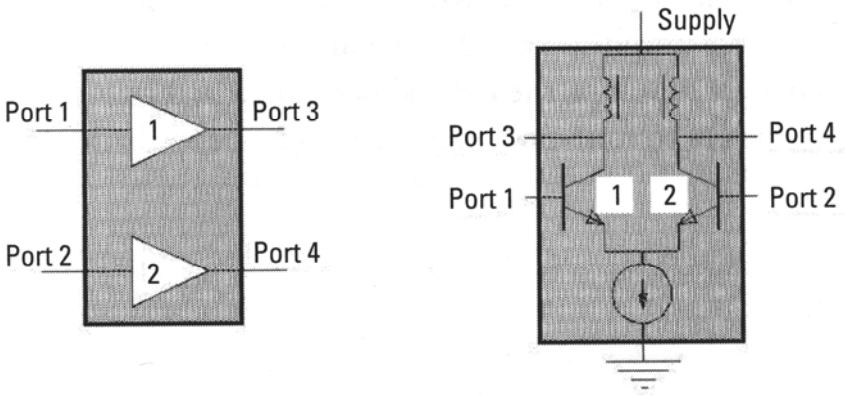

Figure 4: Two DLNA implementations.

There are two basic DLNA implementations (figure 4):

- Two separate amplifiers that are ideally independent and identical (Balanced structure).
- Two amplifying devices with a common-bias current-sink or source.

Both of them are feasible for RF or microwave applications and mixed-mode parameter tools can evaluate both implementations.

1.3.- COTS DLNAs EVALUATED

An exhaustive search of COTS differential low noise amplifiers was undertaken. Only two devices fulfil the bandwidth and noise requirements: CGY2109HV from OMMIC [4] and CDQ0303-OS from MIMIX [5]. Relevant characteristics are described below.

- **CGY2109HV** (OMMIC)
  - Dual MMIC (0.18 um PHEMT process from OMMIC), Isolation = 30 dB
  - Frequency Range: 0.1 to 3.0 GHz
  - 20 dB Gain @1500 MHz
  - 0.6 dB Noise Figure @1500 MHz
  - 11 dBm IIP3
  - S11: -6dB, S22: -14dB for 50 Ohm System
  - Power Supply: 5V, 50 Ma
- **CDQ0303-OS** (MIMIX)

- Matched Pair of pHEMT Transistors for Optimum Balanced Amplifier Design
- Frequency Range: 0.5 to 6.0 GHz
- 25 dB Gain @900 MHz
- 0.6 dB Noise Figure @ 900 MHz
- 33 dBm OIP3
- S11: -3dB, S22: -3.5dB for 50 Ohm System (@ 900 MHz)
- Power Supply: 3V, 50 Ma

As figures 5 and 6 show the functional block diagrams of both DLNAs. Both amplifiers have the same functional diagram (they are balanced type DLNAs).

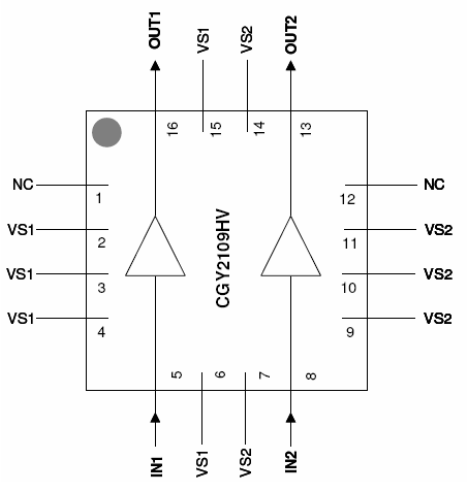

Figure 5: Functional block diagram of the CGY2109HV (OMMIC).

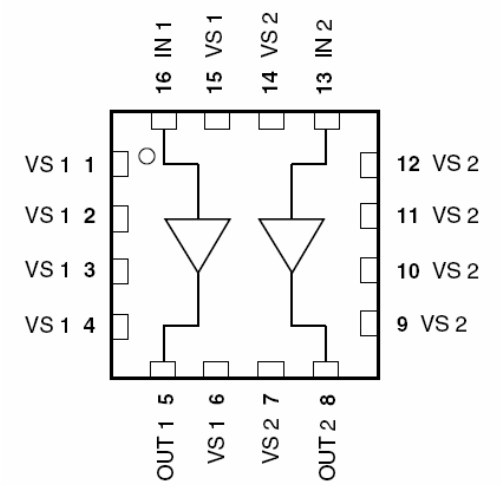

Figure 6: Functional block diagram of the CDQ0303-OS (MIMIX).

1.3.1. – EVALUATION BOARDS

Two evaluation boards were tested for each COTS DLNA tested. One was built in-house and the other was out-sourced.

The in-house evaluation board was designed at ASTRON [8] using a nonlinear model of the CGY2109HV provided by the manufacturer (OMMIC). The schematic diagram is shown in figure 7.

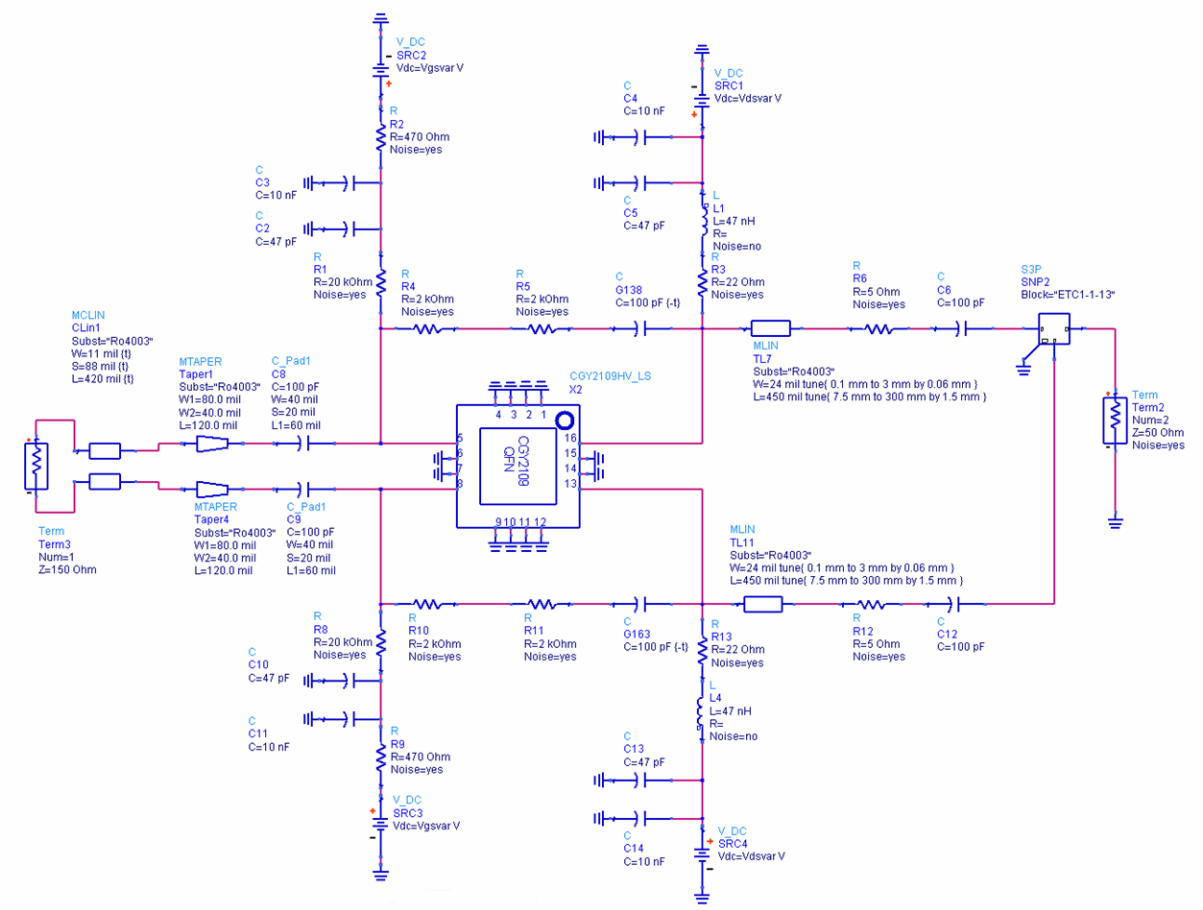

Figure 7: Schematic diagram of the in-house evaluation board with CGY2109HV as DLNA.

The layout and realization of the in-house evaluation board for the CGY2109HV is shown in figure 8 (taken from [8]). The same test board was used for the CDQ0303-OS because of the unavailability of a nonlinear circuit model and it has the same pin-up as the CGY2109HV.

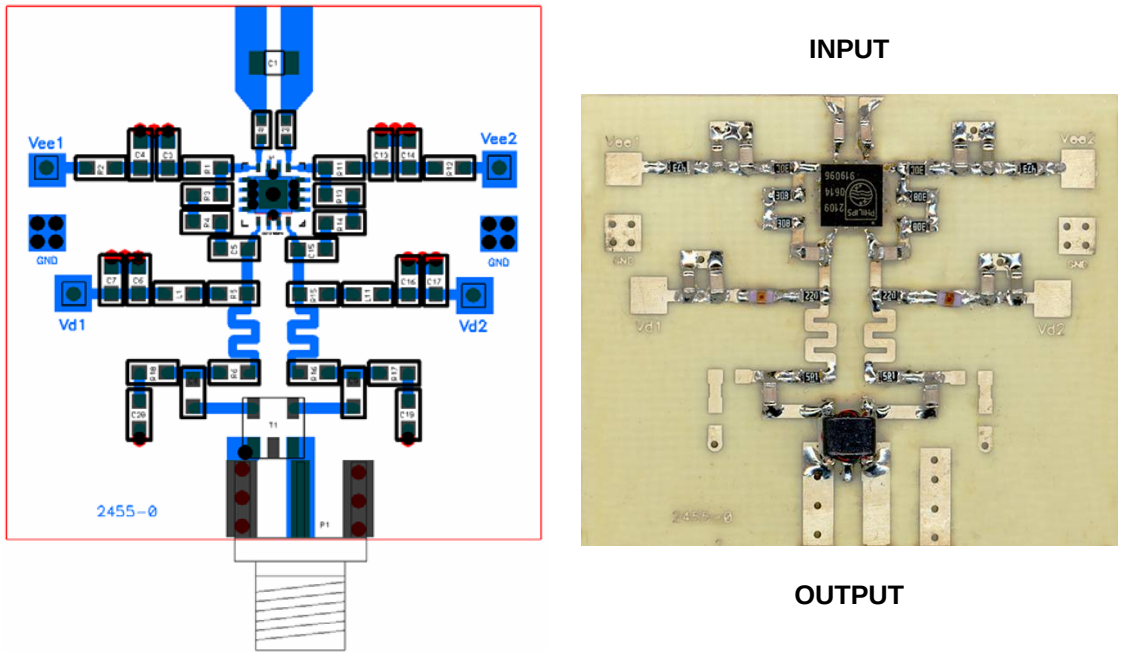

Figure 8: Schematic diagram of the in-house evaluation board with CGY2109HV as DLNA.

The out-sourced evaluation boards were supplied by the manufacturer (OMMIC and MIMIX respectively). Both boards are shown in figure 9.

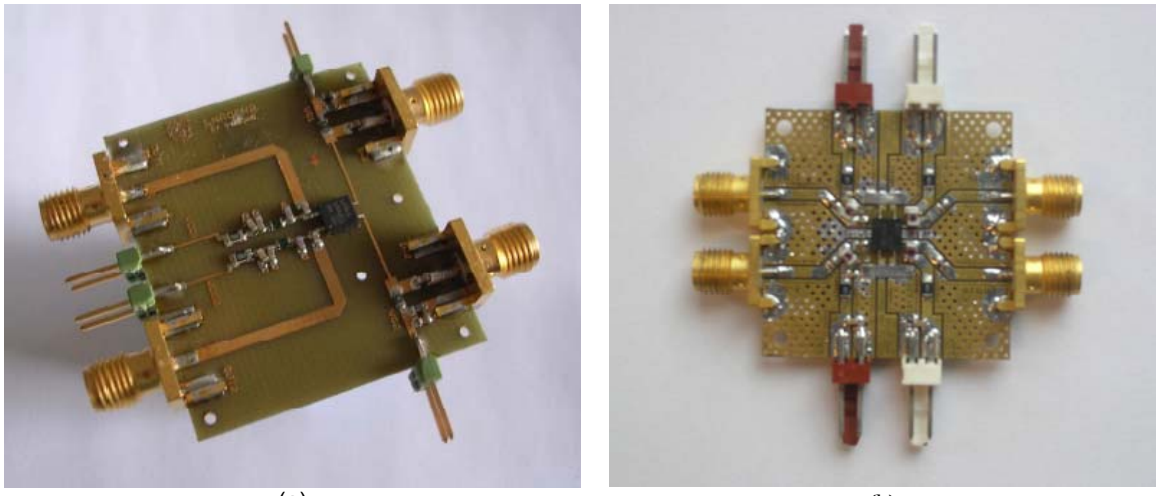

(a) (b)

Figure 9: (a) Out-sourced OMMIC test board (LNAQFN2). (b) Out-sourced MIMIX test board.

1.4.- OUTPUT BALUN TRANSFORMERS

As it is shown on table 1 (system specifications) the output of the active antenna element must be single ended, so a balun was necessary (BALanced to UNbalanced) to connect the output of the DLNA (100 or 150 Ω balanced) to the following circuits (50 Ω single ended).

There are two options for a 100 Ω to 50 Ω conversion:

- A 2:1 transformer
- A 1:1 transformer + an impedance matching network.

An exhaustive search was made of many RF transformers manufacturers: Coilcraft, MA/Com, Mini-circuits, Murata, etc.

- There are *not commercial 2:1 transformers* that fulfil bandwidth requirements (from 300MHz to 1GHz).
- Only MA/COM 1:1 transformers fulfil frequency specifications. **ETC1-1-13** was selected.

The main electrical characteristics of the ETC1-1-13 are shown in table 2:

Parameter	Test Conditions	Frequency	Units	Min	Typ	Max
RF Frequency	—	4.5 - 3000	MHz	—	—	—
Insertion Loss	F_L—f_U	4.5 - 1000 1000 - 2000 2000 - 3000	dB dB dB	— — —	0.32 — —	1.0 2.0 3.5
Amplitude Unbalance	—	4.5 - 1000	dB	—	—	1.0
Phase Unbalance	—	4.5 - 1000	Degrees	—	—	20

Table 2: ETC1-1-13 electrical specifications.

This transformer is a *transmission line* type transformer so there is no DC isolation between primary and secondary (it could increase the noise of the system). The block diagram of the ETC1-1-13 is shown in figure 10:

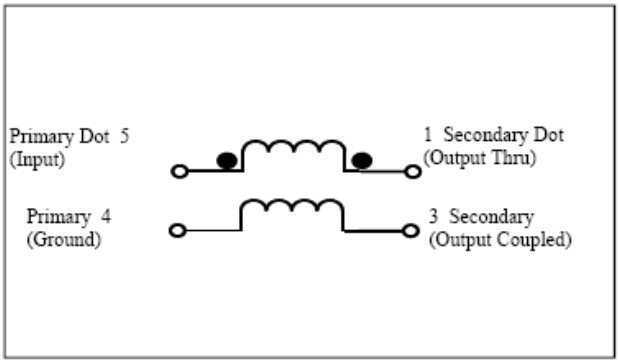

Figure 10: Functional block diagram of the ETC1-1-13 transformer.

Other disadvantage of this solution is that the impedance matching network could be too big in microstrip technology. One option is to design a lossy matching network with discrete elements. In this case, the effect of this network on the noise performance of the amplifier must be evaluated.

2.- MEASUREMENT PROCEDURES

As it was pointed out before, the main disadvantage of the differential devices is that the standard measurement equipment can not be used if it is desired to have a fully differential characterization of the balanced circuit (both in gain and in noise performance).

2.1.- SINGLE-ENDED MEASUREMENTS

Although the low noise amplifiers described in this report are differential, it is interesting to carry out single ended measurements in order to check that the amplifier works properly. These measurements are faster than differential ones so are ideal for a first verification of the performance of the amplifier and for detecting errors.

There are two types of single-ended (S-E) measurements for a DLNA.

1. Single-ended measurements of each channel of the DLNA. Only valid for balanced amplifiers (two channels of single-ended amplifiers).
2. Single-ended measurements using two baluns (one at the input and other at the output of the DLNA). This measurement can be carried out with both types of differential amplifiers.

Figure 11 shows the block diagram for the second type of S-E measurements. The baluns operate as S-E to differential converters and so the standard RF measuring instruments can be used. Nevertheless, there are some difficulties:

- The amplifier gain and noise figure may be de-embedded on the baluns. Mathematical formulas are developed in [6] for this purpose.
- Less accuracy as the baluns are less ideal.
- The frequency range is limited by baluns frequency dependence.

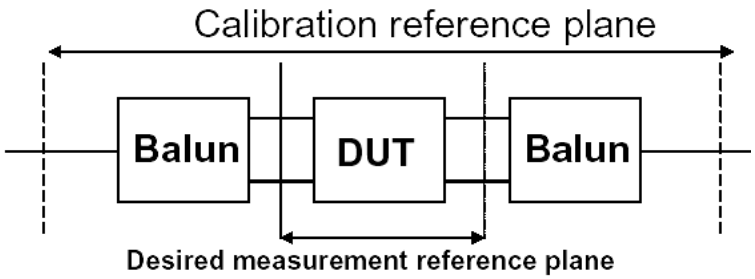

Figure 11: Single ended measurements of a differential amplifier.

Because of these disadvantages only first type of measurements was carried out. These instruments were used:

- The noise figure meter N8975A from Agilent (10 MHz-26.5 GHz).
- The four port vector network analyzer ZVB-20 from Rohde & Schwarz (10 MHz-20 GHz).

2.2.- DIFFERENTIAL MEASUREMENTS

In this case, the noise figure of the DLNA was determined applying the well-known Hot/Cold method to differential configurations [7] using differential loads that operate as differential noise sources.

2.2.1. – NOISE FIGURE DIFFERENTIAL MEASUREMENTS

2.2.1.1. – THE HOT/COLD METHOD

This method is also known as Y factor method and is broadly used to determine the noise performance of S-E devices. It consists on using one resistive load that works as an input noise generator. At the output of the device under test (in this case an amplifier) a power meter is used in order to obtain the output noise power. This power is measured with the load exposed to two different temperatures:

- Hot measurement → normally at ambient temperature (290 K aprox.)
- Cold measurement → the load is dipped into liquid nitrogen (77 K aprox.)

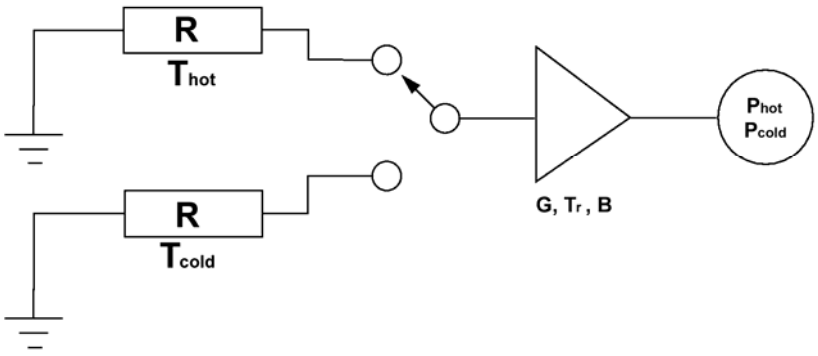

Figure 12: Hot/Cold measurements.

The Y factor is the ratio between the hot and the cold output power:

$$Y = \frac{P_{hot}}{P_{cold}} \tag{1}$$

The system temperature is a measure of the noise generated by the amplifier, and is calculated knowing the Y factor:

$$T_{sys} = \frac{T_{hot} - Y \cdot T_{cold}}{Y - 1} \tag{2}$$

The noise figure is an alternative of the system temperature to evaluate the noise performance:

$$NF(dB) = 10\log\left(\frac{T_{sys}}{T_{hot}+1}\right) \quad (3)$$

The application of this method to differential LNAs consisted of using differential loads. The load resistor of 150 Ω was connected to the PCB via a copper parallel wire line with a characteristic impedance of 150 Ω, in order to keep thermal coupling between the load and the LNA as small as possible. PTFE supports were used to keep the wires separated.

The output of the DLNA must be single-ended in order to use a standard spectrum analyzer to measure the output noise power. For this reason, a balun transformer is placed at the differential output of the chip in the in-house evaluation board (see figure 8).

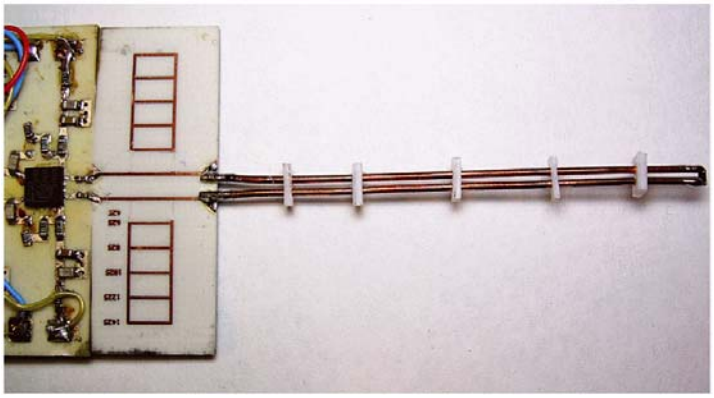

Figure 13: Implementation of the differential load.

2.2.1.2. – DIFFERENTIAL LOAD

2.2.1.2.1. – DESIGN AND SIMULATIONS

In this section, the design procedure of the differential load is explained. First of all, theoretical formulas were used to design them. Because of the bad first results obtained, a simulation using HFSS were carried out in order to improve this design.

The geometry of the differential load is too simple as it is shown in figure 14. It consists on two parallel copper wires which characteristics are:

- Diameter $d = 2a$ = 0.8 mm
- Copper:
  - σ = 5.813 E -7 S/m (electrical conductivity)
  - ρ = 1.72 E-8 Ω·m (electrical resistivity)

The design parameter is the spacing *D* between wires.

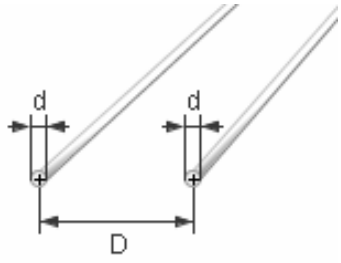

Figure 14: Differential load geometry.

FIRST APPROACH (Using theoretical formulas)

The classical transmission line model of the parallel wires lines (also known as Lecher lines) was used. For more accuracy lossless line approximation was not used. In this case, the transmission line parameters and the geometrical parameters of the Lecher lines are related by the following equations [9]:

- Resistance per unit length:

$$R = \frac{1}{\pi \cdot a \cdot \sigma_{cond} \cdot \delta} \tag{4}$$

- Inductance per unit length:

$$L = \frac{\mu}{\pi} \cosh^{-1}\left(\frac{D}{2a}\right) \tag{5}$$

- Conductance per unit length:

$$G = \frac{\pi \cdot \sigma_{diel}}{\cosh^{-1}\left(\frac{D}{2a}\right)} \tag{6}$$

- Capacitance per unit length:

$$C = \frac{\pi \cdot \varepsilon}{\cosh^{-1}\left(\frac{D}{2a}\right)} \tag{7}$$

Where δ is the skin depth:

$$\delta = \sqrt{\frac{1}{\pi \cdot \mu \cdot f \cdot \sigma_{cond}}} \tag{8}$$

The characteristic impedance of the transmission line is determined by:

$$Z_0 = \sqrt{\frac{R + j\omega L}{G + j\omega C}} \tag{9}$$

Figure 15 shows the characteristic impedance versus *D* for a design frequency of 800 MHz. The imaginary part of Z_0 is -0.175 for all distances.

For the copper wires used, a spacing of $\boxed{D = 1.512 \ \ mm}$ gives a characteristic impedance near to the desired 150 Ω. The actual the characteristic impedance is:

$$Z_0 = 150.014 - j0.175\ [\Omega] \qquad (10)$$

Differential loads with different lengths (25, 50, 75 and 100 mm) were built. The input impedance measured using a standard VNA is shown in figures 16 and 17 (real and imaginary part respectively).

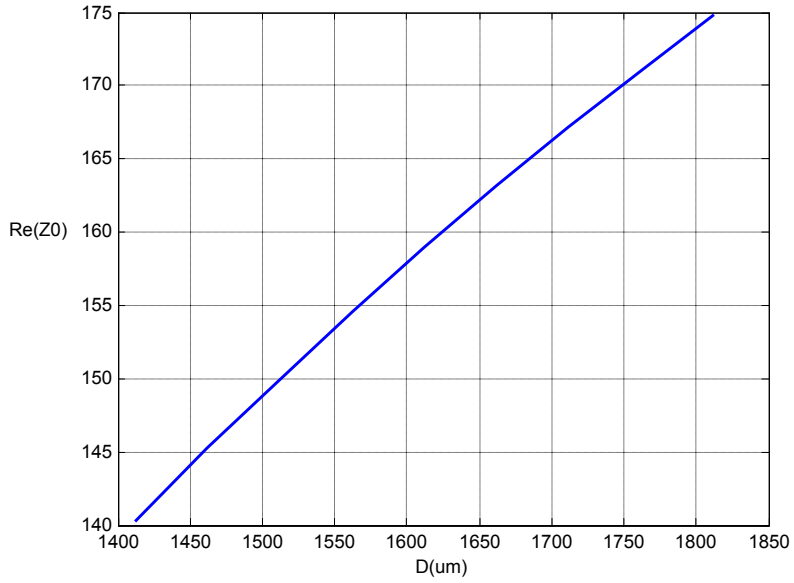

Figure 15: Characteristic impedance versus spacing.

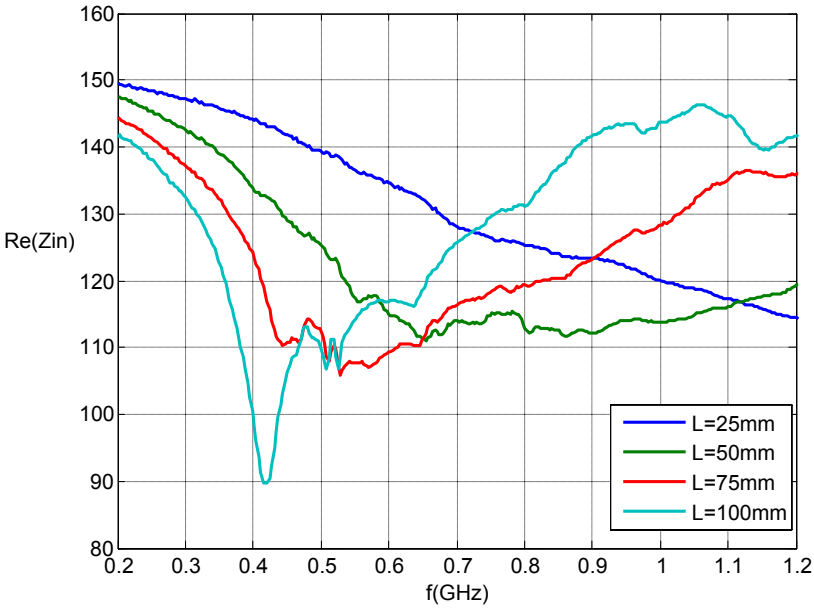

Figure 16: Measurements results of the real part for the input impedance of the differential load (first approach).

Comments:

- As the length increases, the results deteriorate.
  - For 25 mm → 120 Ω < Re(Zin) < 148 Ω (in our interest band)
  - For 100 mm → 90 Ω < Re(Zin) < 145 Ω (in our interest band)
  - A strange resonance appears near 420MHz for the 100mm line.
- Better results were expected.

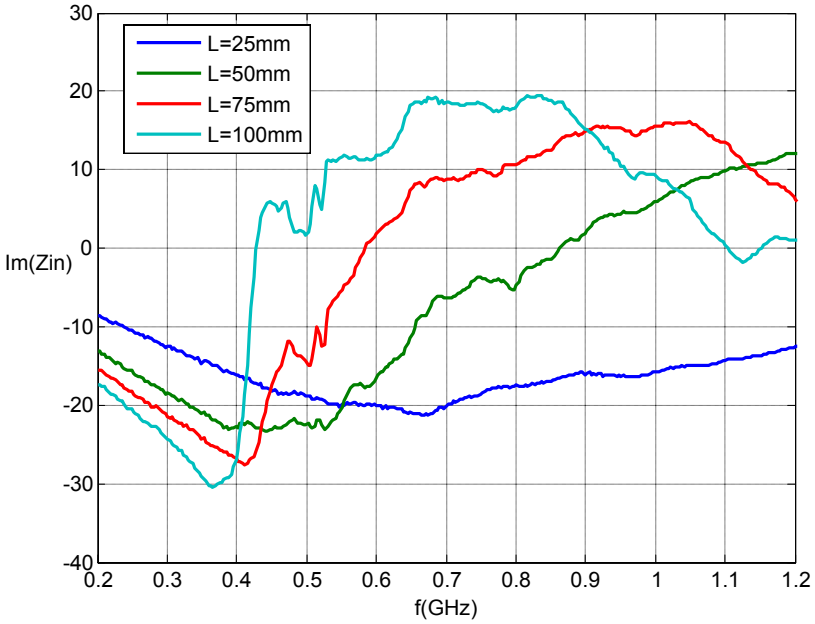

Figure 17: Measurements results of the imaginary part for the input impedance of the differential load (first approach).

SECOND APPROACH (Simulation with HFSS)

As the measurements of the differential loads designed using theoretical formulas were not acceptable (distance between loads 1512 um), new loads were designed using the electromagnetic simulator HFSS.

The model is shown in figure 18. A wave-port of 150 Ω was used as terminal load and another of 50 Ω was used for input reference.

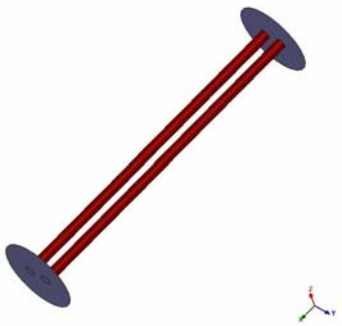

Figure 18: HFSS model of the differential load.

In the first approach, the design parameter was the characteristic impedance. However, to achieve a good input matching, an *input impedance* of 150 Ω is required. Therefore, in this simulation, the input parameter was chosen as design parameter.

For a length of 25mm, the distance between wires was varied in order to find the optimum value for a desired 150 Ω. The simulation results are shown in figures 19 and 20.

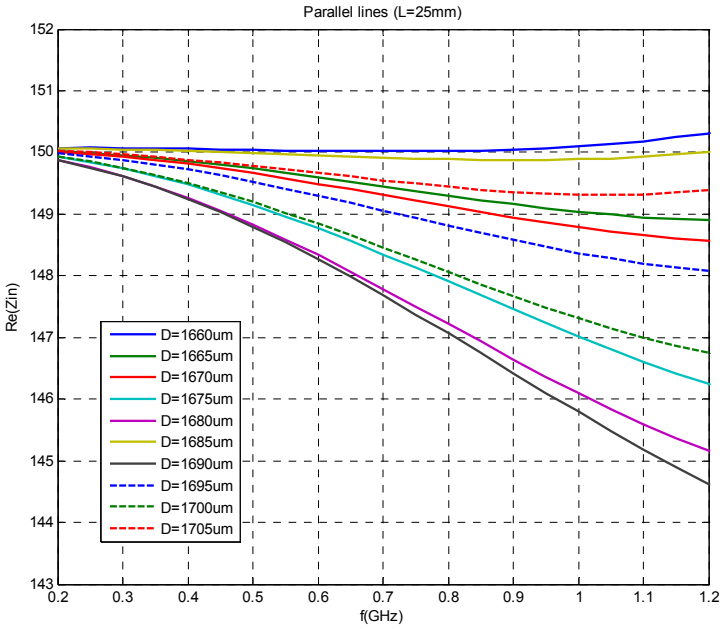

Figure 19: HFSS simulations of the real part for the input impedance of a differential load (L=25 mm).

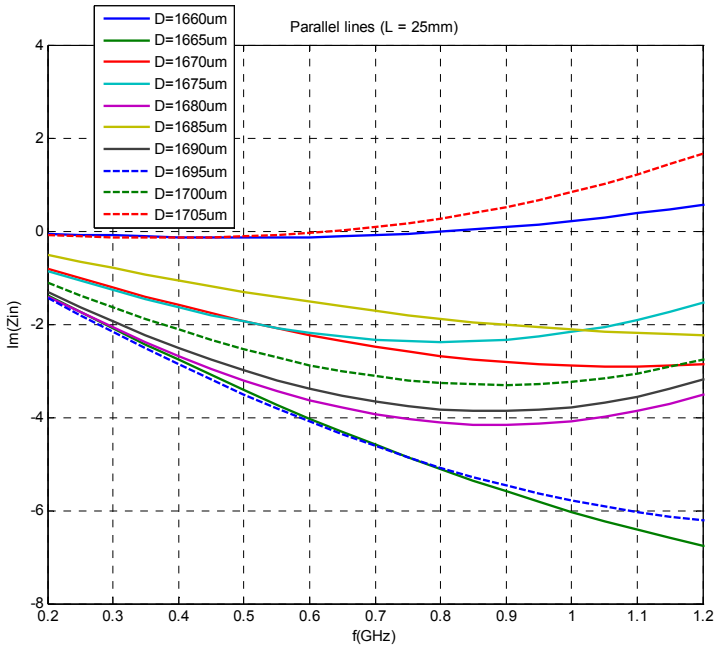

Figure 20: HFSS simulations of the imaginary part for the input impedance of a differential load (L=25 mm).

The input impedance is closest to 150 Ω for the spacing D values:

- D = 1660 um
- D = 1685 um

Effects of the wires' length.

For the chosen values, a new simulation was run in order to check the effect of the wires' length. The length values were 25, 50, 75 and 100 mm.

- **D = 1660 um**

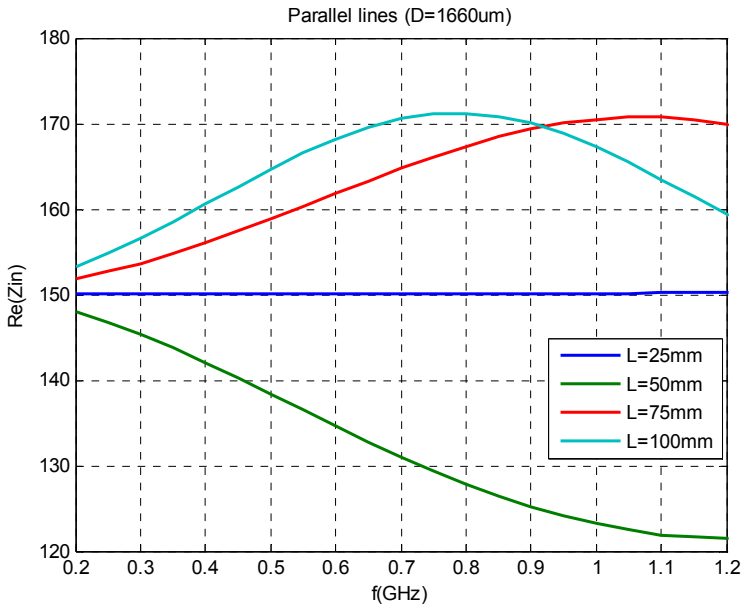

Figure 21: HFSS simulations of the real part for the input impedance of different lengths differential loads (D=1660 um).

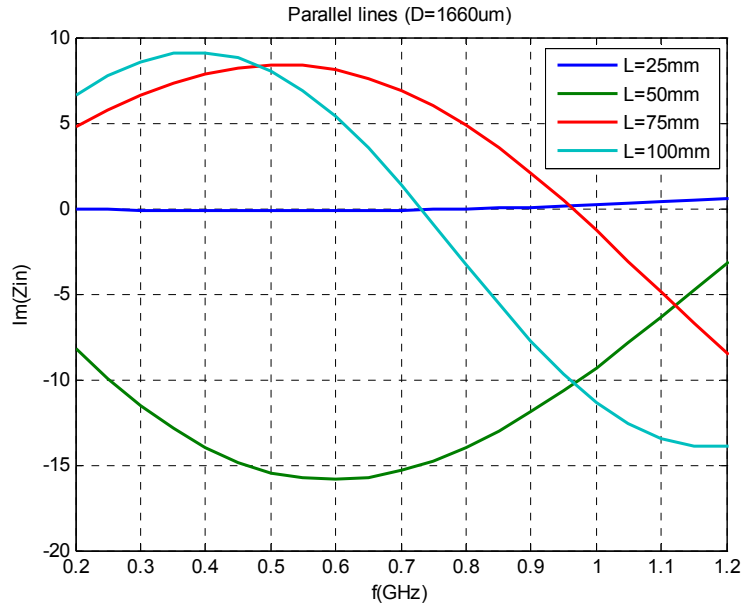

Figure 22: HFSS simulations of the imaginary part for the input impedance of different lengths differential loads (D=1660 um).

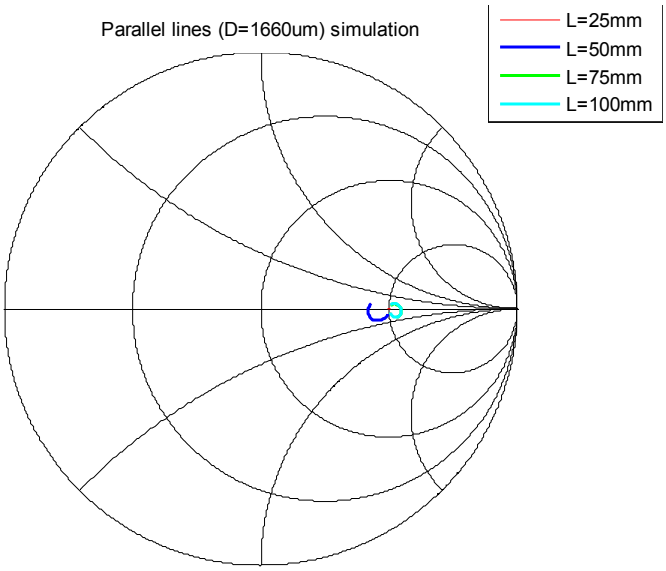

Figure 23: HFSS simulations of the input impedance for different length differential loads (D=1660 um). A Smith chart with a 50 Ω reference is used.

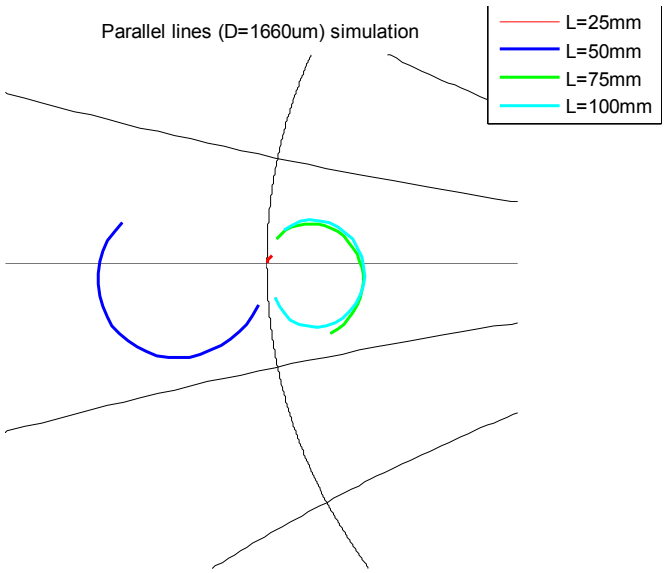

Figure 24: HFSS simulations of the input impedance for different length differential loads (zoom).

- **D = 1685 um**

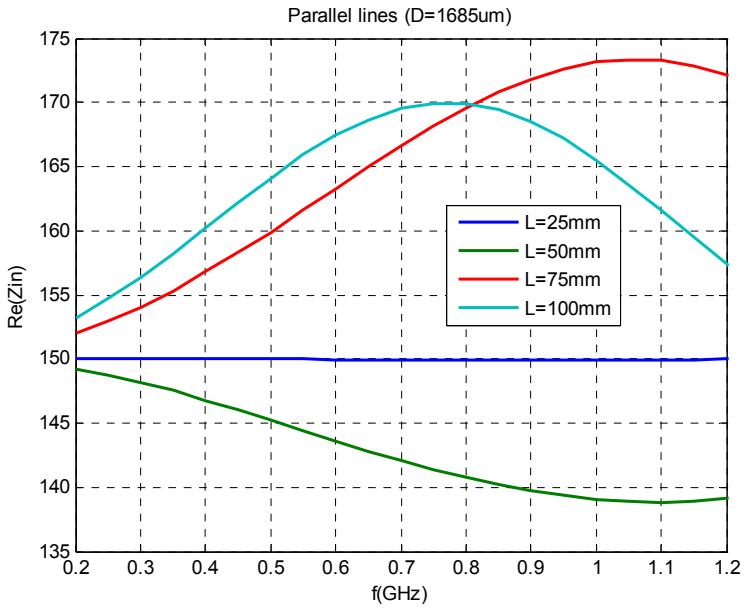

Figure 25: HFSS simulations of the real part for the input impedance of different lengths differential loads (D=1685 um).

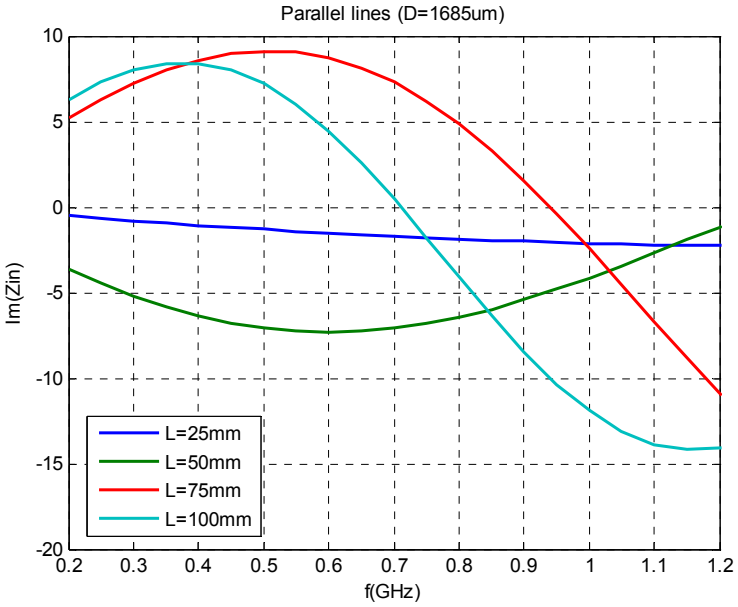

Figure 26: HFSS simulations of the imaginary part for the input impedance of different lengths differential loads (D=1685 um).

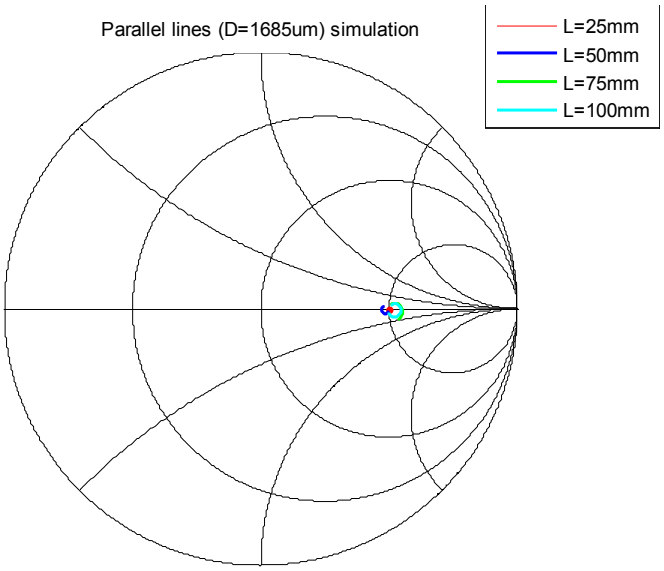

Figure 27: HFSS simulations of the input impedance for different length differential loads (D=1685 um). A Smith chart with a 50 Ω reference is used.

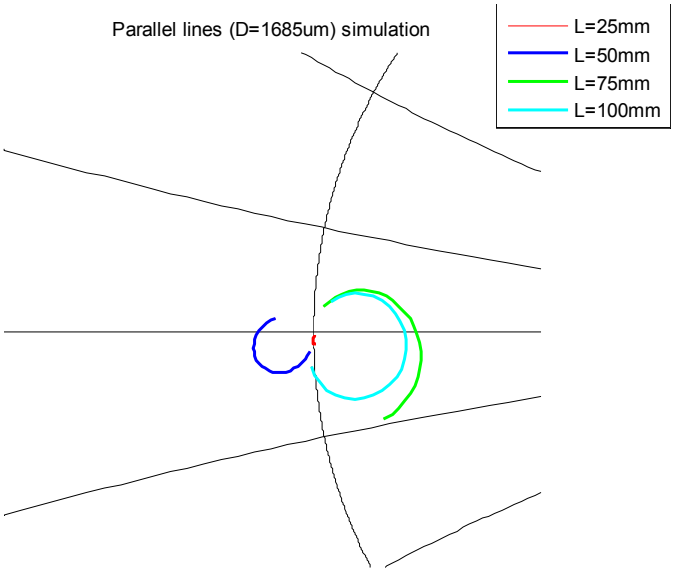

Figure 28: HFSS simulations of the input impedance for different length differential loads (Smith chart).

Seeing figures 23 and 27, **1685 um** was built, because the curves are closer to 150 ohms.

2.2.1.2.2. – MEASUREMENTS

Differential loads were built (D=1685 um) for lengths of 25, 50, 75 and 100 mm. Different lengths were chosen in order to study the effect of the variation of the lengths on the noise performance of the DLNAs evaluated.

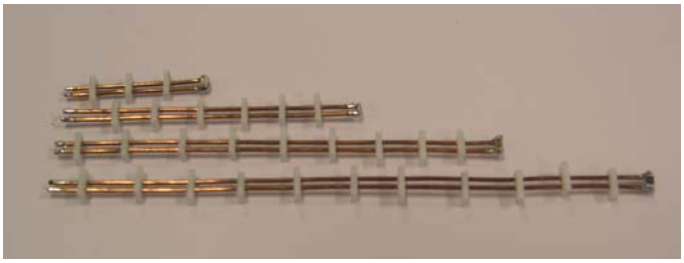

Figure 29: Differential loads.

To check the performance of each differential load, some measurements were done using a VNA and a TDR (Time Domain Reflectometer).

- **VNA MEASUREMENTS**

Impedance was measured for each differential load using a HP 8753D VNA. The SMA connector used was also calibrated.

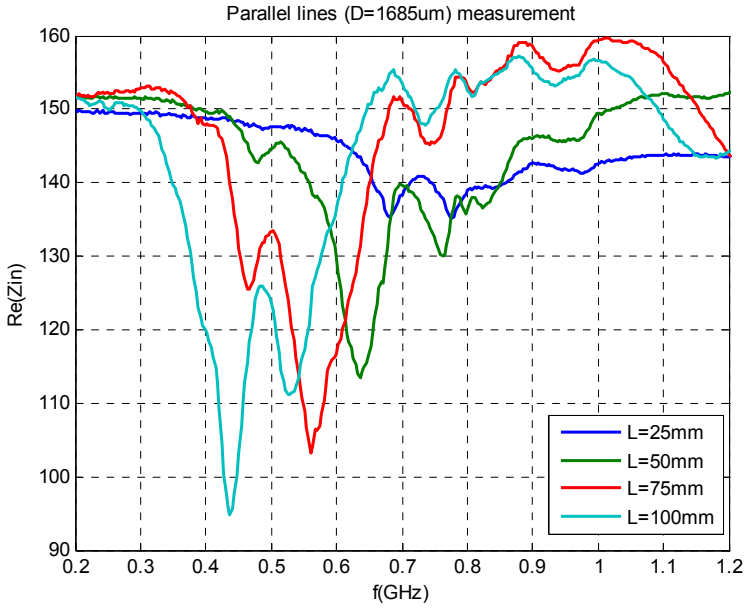

Figure 30: VNA measurements of the real part for the input impedance of different length differential loads (D=1685 um).

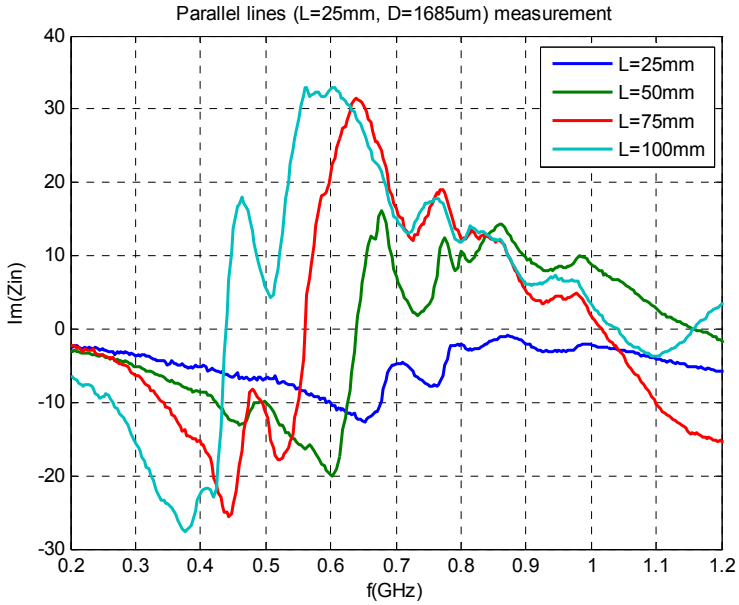

Figure 31: VNA measurements of the imaginary part for the input impedance of different length differential loads (D=1685 um).

A big resonance appears in the impedance curve (see figure 30) for all loads except for the 25 mm load (the shortest one). It could be due to the PTFE supports effects that are no taken into account in the simulation (as the length increases more Teflon pieces are needed). Also it could be a mismatch issue due to the transition between the differential load and the SMA connector used to carry out the VNA measurements.

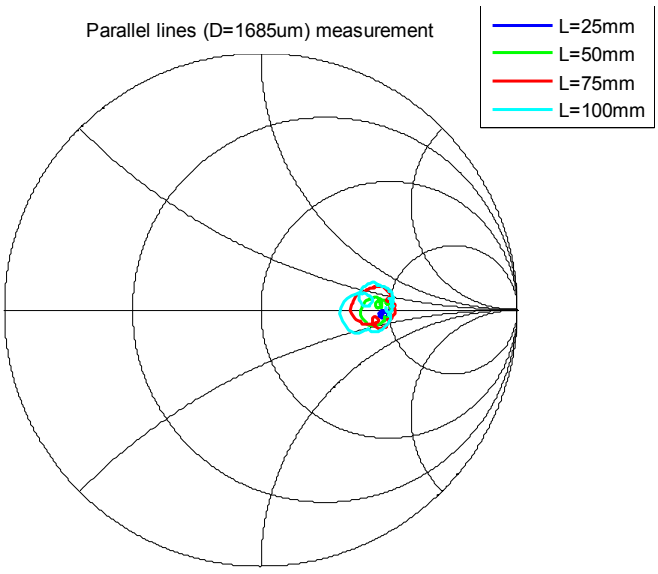

Figure 32: VNA measurements of the input impedance for different length differential loads (D=1685 um). A Smith chart with a 50 Ω reference is used.

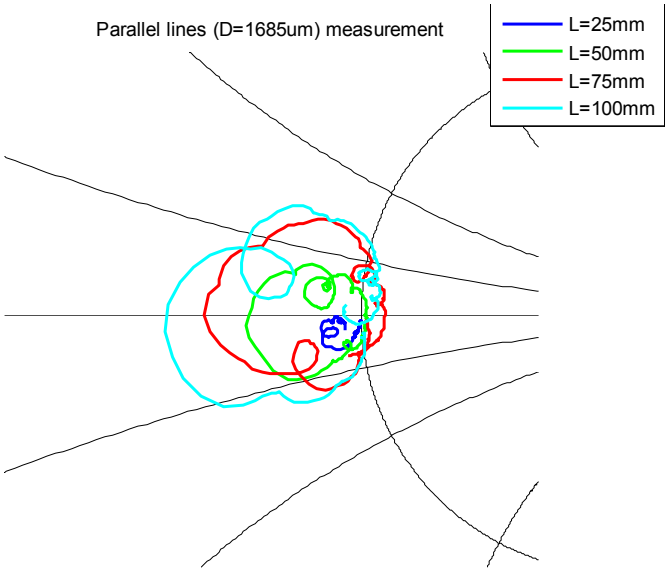

Figure 33: VNA measurements of the input impedance for different length differential loads (Smith chart).

Results are better than with the old loads (first approach design), because the impedance is closer to 150 Ω. As figure 33 shows, the best result is achieved with a length of 25 mm, which is our design length.

- **TDR MEASUREMENTS**

Several experiments were carried using the 54754A differential Time Domain Reflectometer module integrated on the 86100B oscilloscope (both from Agilent).

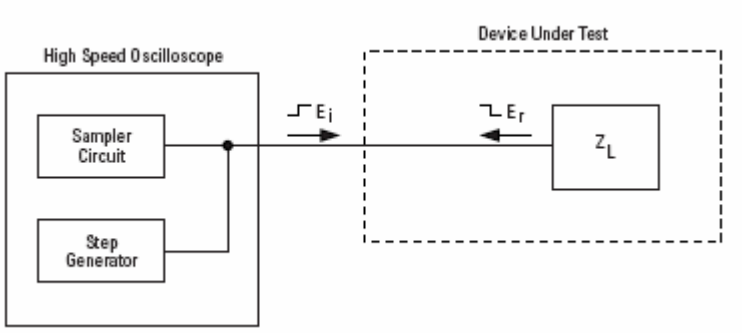

Figure 34: Functional block diagram for a TDR module.

A TDR setup is shown in figure 34. The step generator produces a forward-going incident wave that is applied to the transmission system under test. The step travels down the transmission line at the velocity of propagation of the line. If the load impedance is equal to the characteristic impedance of the line, no wave is reflected and all that will be seen on the oscilloscope is the incident voltage step recorded as the wave passes the point on the line monitored by the oscilloscope.

If a mismatch exists at the load, part of the incident wave is reflected. The reflected voltage wave will appear on the oscilloscope display algebraically added to the incident wave. Refer to Figure 35.

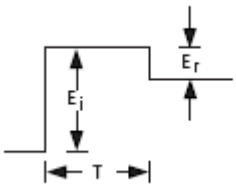

Figure 35: Oscilloscope display when Er ≠ 0.

For these measurements the 50 mm differential load was used. Teflon pieces were used to keep the distance between wires. The effect of this PTFE pieces in the impedance measurements was evaluated on these experiments. For this purpose, some experiments, changing the position of these pieces, were conducted.

VARYING THE POSITION OF THE TEFLON PIECES

First of all, some test were conducted by varying the position of the Teflon pieces using the oldest differential load (*D* = 1.512 mm), designed using theoretical formulas. Notice that the characteristic impedance measured is near 140 Ω.

- ***Equal-spacing pieces***

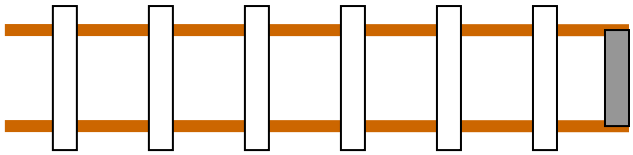

Figure 36: Differential load with Teflon support pieces (equal spacing pieces).

A screen capture from the 86100 oscilloscope is shown in figure 37. This waveform is the sum of the incident pulse and the reflected voltages measure at the same point. This shape depends on the reflection coefficient at every point of the transmission line. Therefore, the impedance profile along the line can be obtained.

The markers point at the impedance at the input of the differential load and at the first Teflon piece location, respectively. Also distances were estimated thought the pulse transit time (D = c·T/2), assuming $\varepsilon_r = 1$. In table 1, some impedance values are shown.

The negative bump (capacitive) is consequence of the termination resistors load. Maybe it is also possibly due to a bad soldered joint.

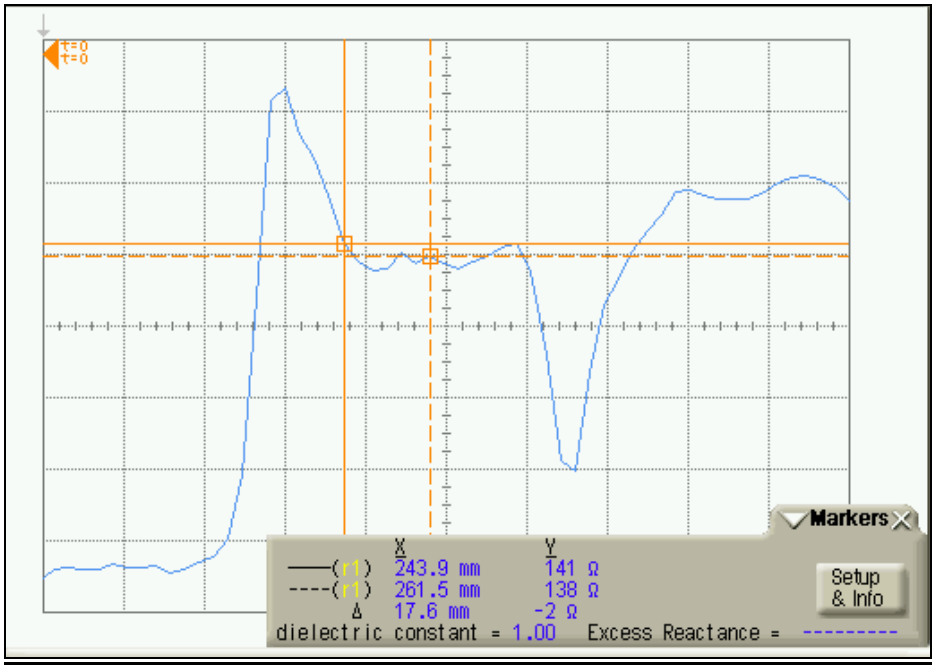

Figure 37: TDR measurements of the characteristic impedance for a 150 Ω differential load.

Interest point	*Distance*	*Impedance*
Line input	0 mm	141 Ω
First Teflon piece	17.6 mm	138 Ω
Last Teflon piece	35.1 mm	140 Ω
Load transition	43.9 mm	112 Ω

Table 2: Results for TDR measurements (equal-spacing pieces).

- ***All pieces together at the centre of the line***

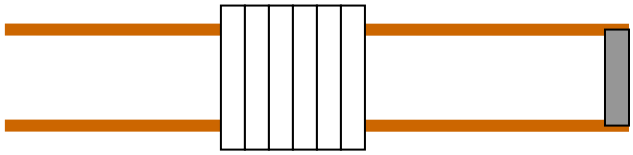

Figure 38: Differential load with Teflon support pieces (all together at the centre of the line).

A negative spur appears because of the effect of the Teflon block. The impedance decreases to 127 Ω.

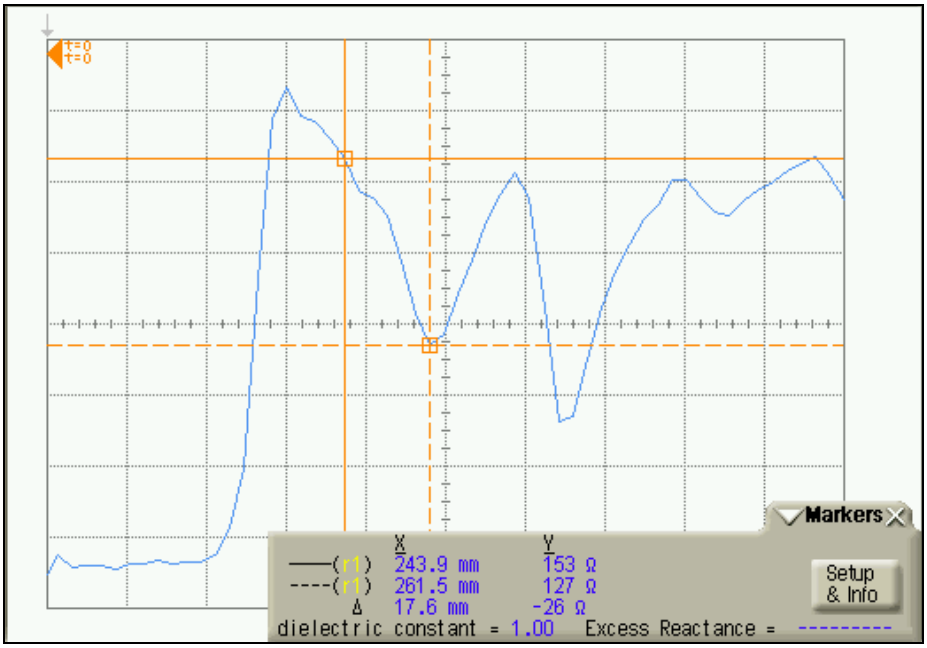

Figure 39: TDR measurements of the characteristic impedance for a 150 Ω differential load.

Interest point	*Distance*	*Impedance*
Line input	0 mm	153 Ω
Teflon pieces block	17.6 mm	127 Ω

Table 3: Results for TDR measurements (all together at the centre of the line).

- ***Two equal-spacing blocks of three pieces***

Figure 40: Differential load with Teflon support pieces (two equal spacing blocks).

Interest point	*Distance*	*Impedance*
Line input	0 mm	144 Ω
First Teflon pieces block	8.8 mm	129 Ω
Second Teflon pieces block	26.9 mm	128 Ω

Table 4: Results for TDR measurements (two equal spacing blocks).

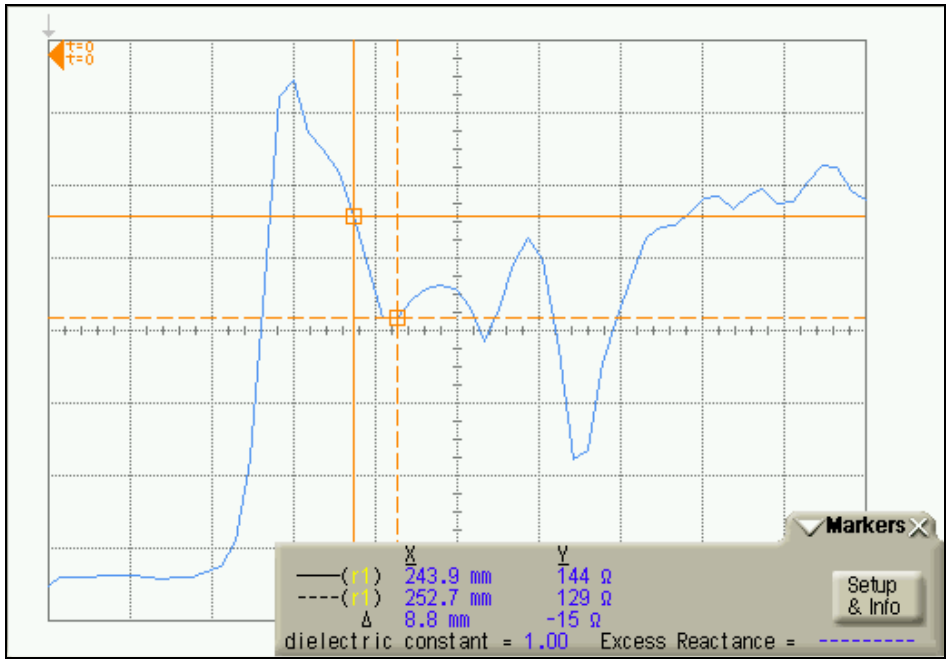

Figure 41: TDR measurements of the characteristic impedance for a 150 Ω differential load.

- ***Three equal-spacing blocks of two pieces***

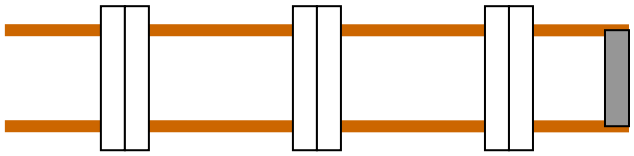

Figure 42: Differential load with Teflon support pieces (three equal spacing blocks).

Interest point	*Distance*	*Impedance*
Line input	0 mm	141 Ω
First Teflon pieces block	2.9 mm	136 Ω
Second Teflon pieces block	17.6 mm	135 Ω
Third Teflon pieces block	32.2 mm	134 Ω

Table 5: Results for TDR measurements (two equal spacing blocks).

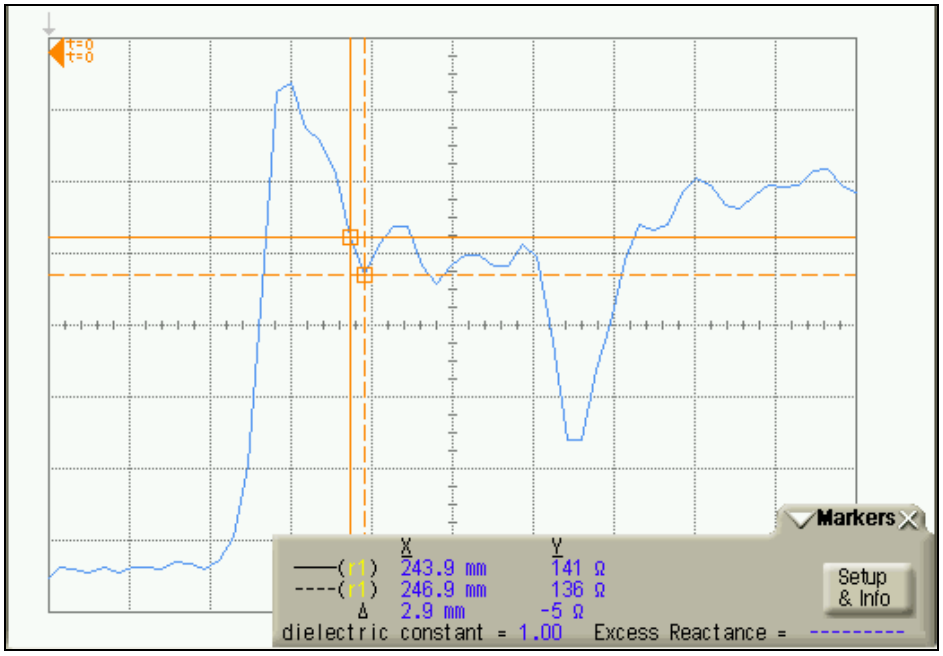

Figure 43: TDR measurements of the characteristic impedance for a 150 Ω differential load (three equal spacing blocks).

CONCLUSIONS:

- The effect of Teflon pieces was studied. These discontinuities have capacitive behaviour, and produce an impedance decreasing.
- So it is interesting to use the minimum number of supports that keep the distance between wires. Six pieces are too many for 50 mm wires. Probably three equal-spacing Teflon pieces are enough.
- TDR measurements are useful to make characteristic impedance measurements and to detect discontinuities along the transmission line. It only provides stationary values of impedance, because it only gives the step response of the differential circuit.

TDR MEASUREMENTS WITH THE DIFF. LOADS DESIGNED USING HFSS

New TDR measurements were done in order to check the value of the characteristic impedance for the differential loads designed using HFSS (second approach). The number of Teflon supports was reduced (3 instead of 6) to improve the performance. Figure 45 shows the waveform in a case of equal spacing Teflon pieces. The characteristic impedance is 148.7 Ω and the Teflon pieces have the same effect as in the previous measurements (capacitive behaviour).

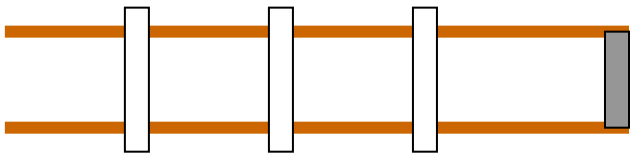

Figure 44: Differential load with Teflon support pieces.

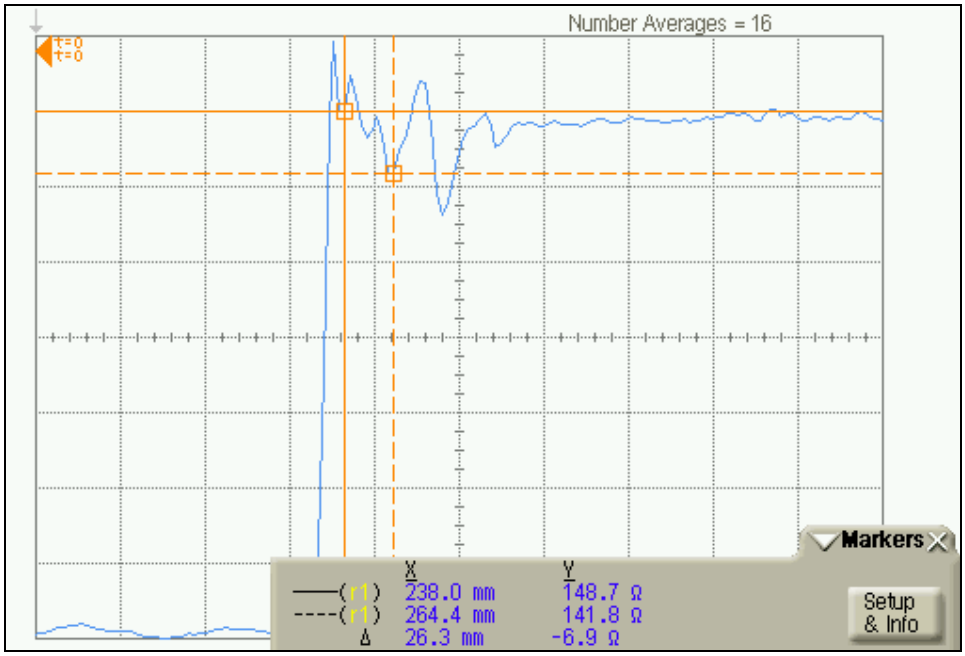

Figure 45: TDR measurements for the characteristic impedance of a 150 Ω differential load.

CONCLUSIONS:

- HFFS design procedure is more accurate that theoretical method.
- Impedance measurements results are close to 150 Ω.

2.2.1.2. – HOT/COLD MEASUREMENTS SET-UP

It is necessary for carrying out the hot/cold method measurements:

- A Differential load (25 mm in the first experiment) that operates as noise source.
- A recipient filled by Liquid Nitrogen (77 K) in which the differential load must be immersed for the cold measurement.
- An amplifier (to increase the noise floor of the system).
- A Spectrum analyzer (8562FC Agilent) to measure the noise power.

Therefore, the output of the differential device under test was connected to the input of the single amplifier, and the output of this to the spectrum analyzer. The set-up is shown in figure 46.

The experiment was carried out in the ASTRON Faraday cage in order to minimize RFI effects.

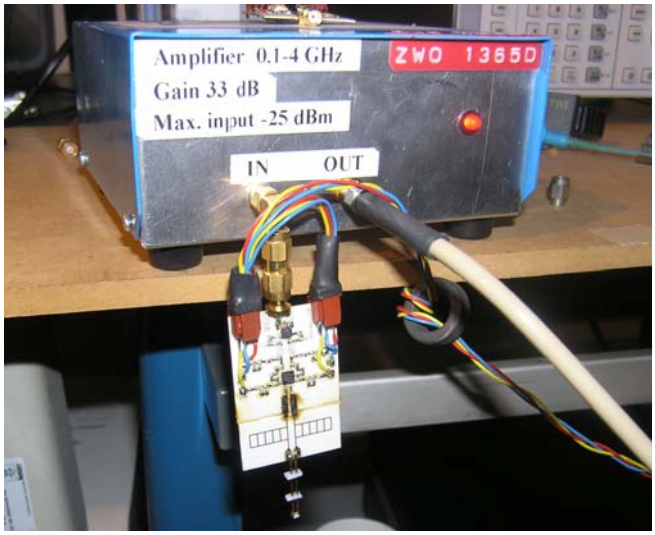

(a)

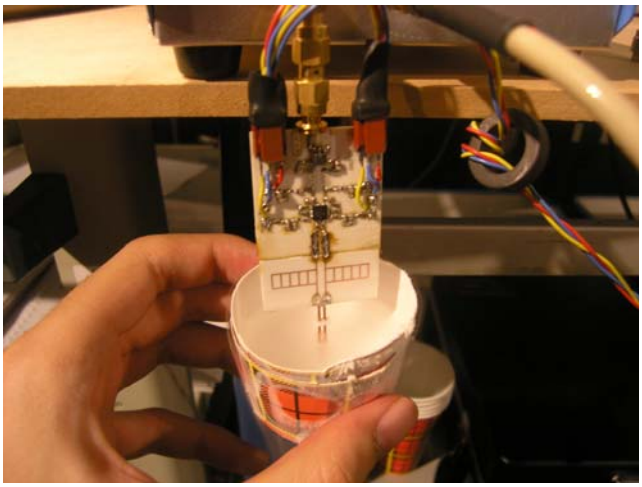

(b)

Figure 46: Hot-cold measurements set-up

3.- MEASUREMENT RESULTS

Practical results are presented in this section. As it was pointed before, two COTS DLNA were evaluated: CGY2109HV from OMMIC and CDQ0303-OS from MIMIX. For both DLNAs two evaluation board were tested.

3.1.- CGY2109HV (OMMIC)

Two evaluation boards were tested. One was built in-house and the other was out-sourced.

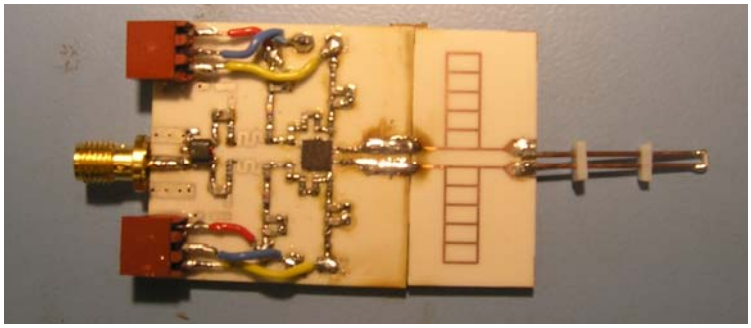

Figure 47: In-house OMMIC test board.

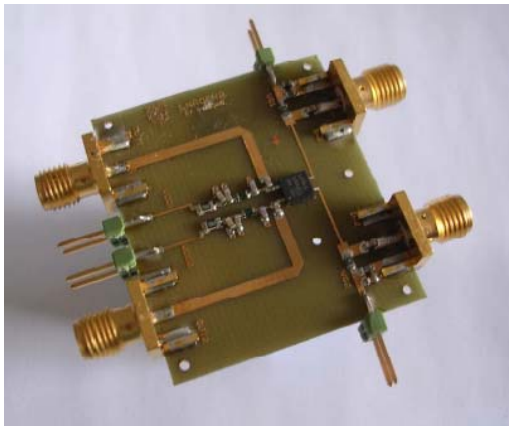

Figure 48: Out-sourced OMMIC test board (LNAQFN2).

3.1.1.– SINGLE ENDED MEASUREMENTS

3.1.1.1. – IN-HOUSE OMMIC EVALUATION BOARD

Both channel of the in-house evaluation board were evaluated. Both gain and noise figure are shown in figure 49, 50 and 51 for different bias points.

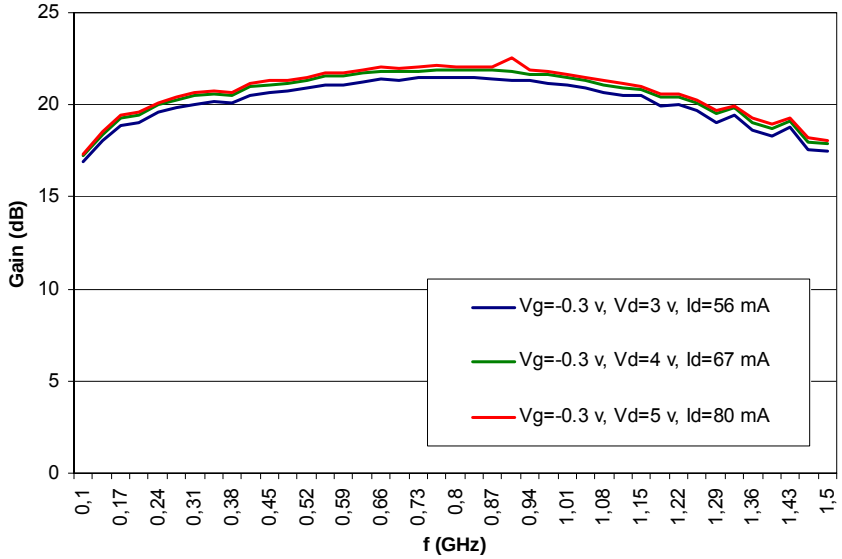

Figure 49: Gain for the in-house OMMIC test board.

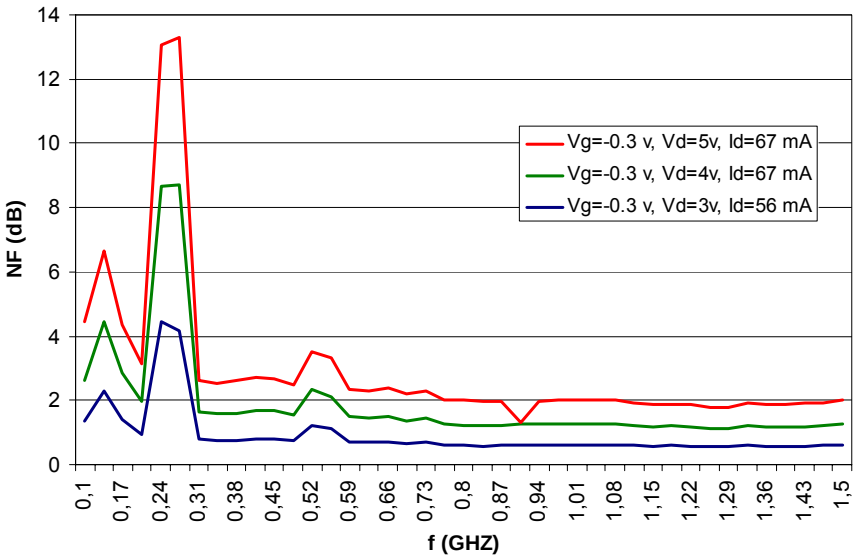

Figure 50: Noise figure for the in-house OMMIC test board.

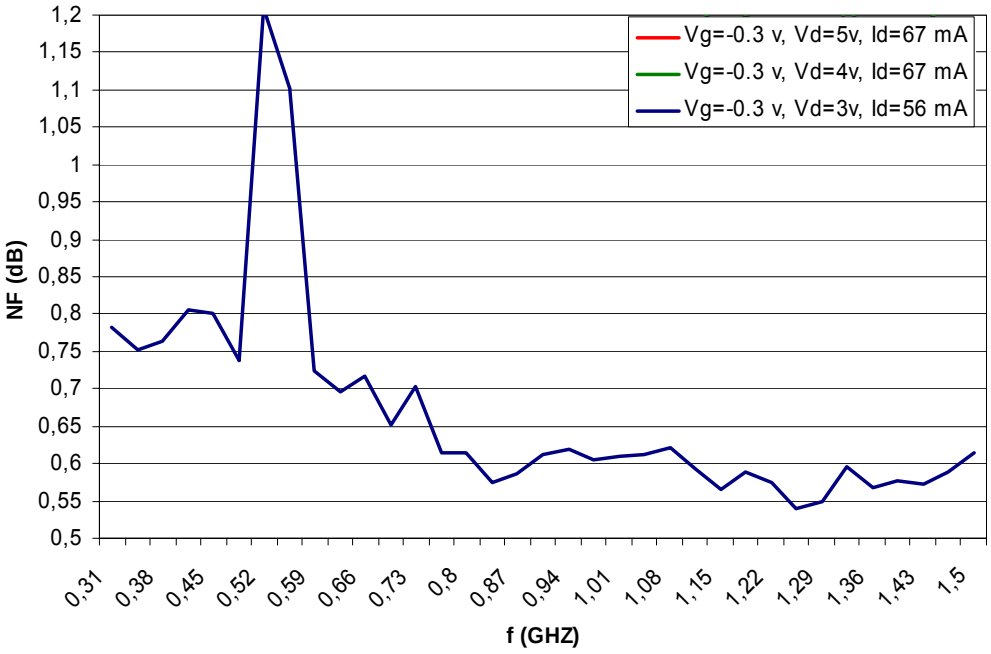

Figure 51: Noise figure for the in-house OMMIC test board (zoom).

The best results are achieved with a gate voltage of -0.3 V. and a drain voltage of 3 V. (drain current of 56 mA per channel). At 700 MHz the gain is 21.3 dB and the noise figure is 0.625 dB.

The noise peak around 200 MHz appears in all the measurements done with this noise figure meter. Doing measurements in the Faraday cage (an EMC shielded test room); we notice that this peak disappeared if the display of the noise figure meter is switched off.

3.1.1.2. – OUT-SOURCED OMMIC EVALUATION BOARD

A test board provided by OMMIC was tested. Figure 52 and 53 shows the gain and noise figure of the DLNA measured with the noise figure meter N8975A from Agilent. They are shown for the following bias points:

- BIAS 1:
  - Vg = -0.3 V
  - Vd = 3 V
  - Id = 60 mA per channel
- BIAS 2:
  - Vg = -0.4 V
  - Vd = 3 V
  - Id = 43 mA per channel

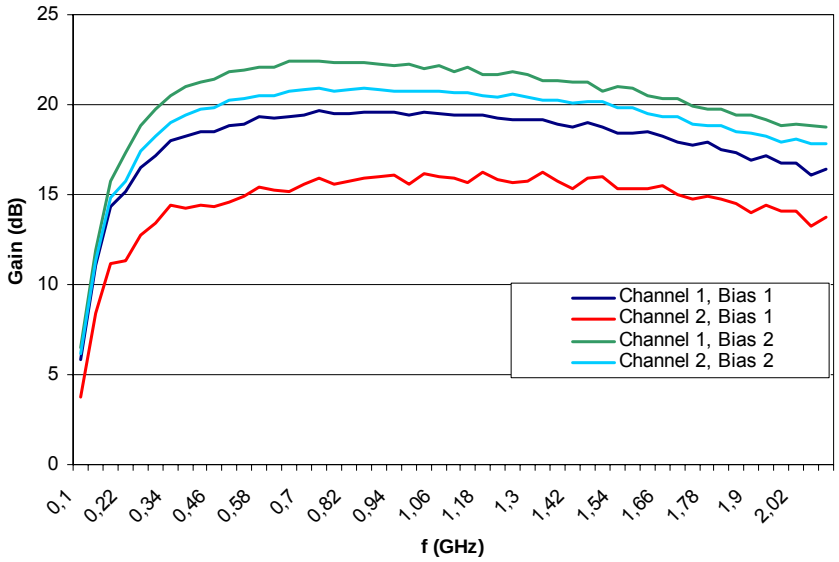

Figure 52: Gain for the out-sourced OMMIC test board (LNAQFN2).

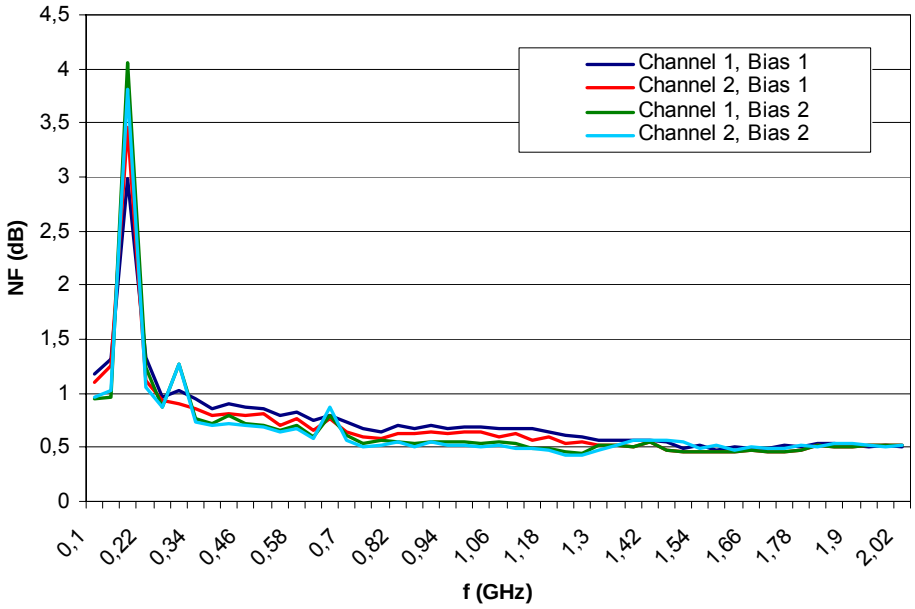

Figure 53: Noise Figure for the out-sourced OMMIC test board (LNAQFN2).

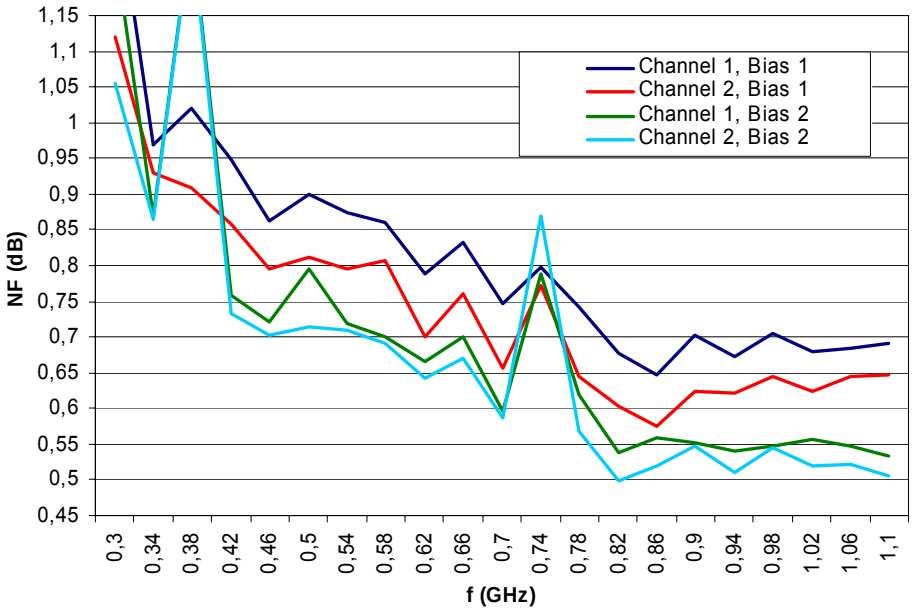

Figure 54: Noise Figure for the out-sourced OMMIC test board (zoom).

The results are better for BIAS 2. In the PACMAN frequency band, the gain is around 22 dB and the noise figure is around 0.6 dB. It must be taken into account that the out-sourced evaluation board is optimized for an application at 1950 MHz. Also there is a difference in gain of 2 dB for bias 1 and 4 dB for bias 2 between the two channels of the differential amplifier. Again, a spike appears near 200 MHz in the noise curve (generated by the noise figure meter).

On the other hand, figure 55 shows the standard s-parameters measured using the 4-port VNA ZVB-20 from Rohde-Schwarz. The bias point for this measurement is Vg=−0.3 V. and Vd = 3 V. There is a difference of 2 dB in gain between the two channels as we have seen in previous single-ended measurements with the noise figure meter. Also notice that the input reflection coefficient for both channels (s_{11} and s_{33} parameters) is too poor.

The s-parameters for the channel 1 (ports 1 and 2) are shown in figure 56. The forward gain is around 15 dB within the required bandwidth (300MHz-1GHz). However the input reflection coefficient is too bad (near 0 dB).

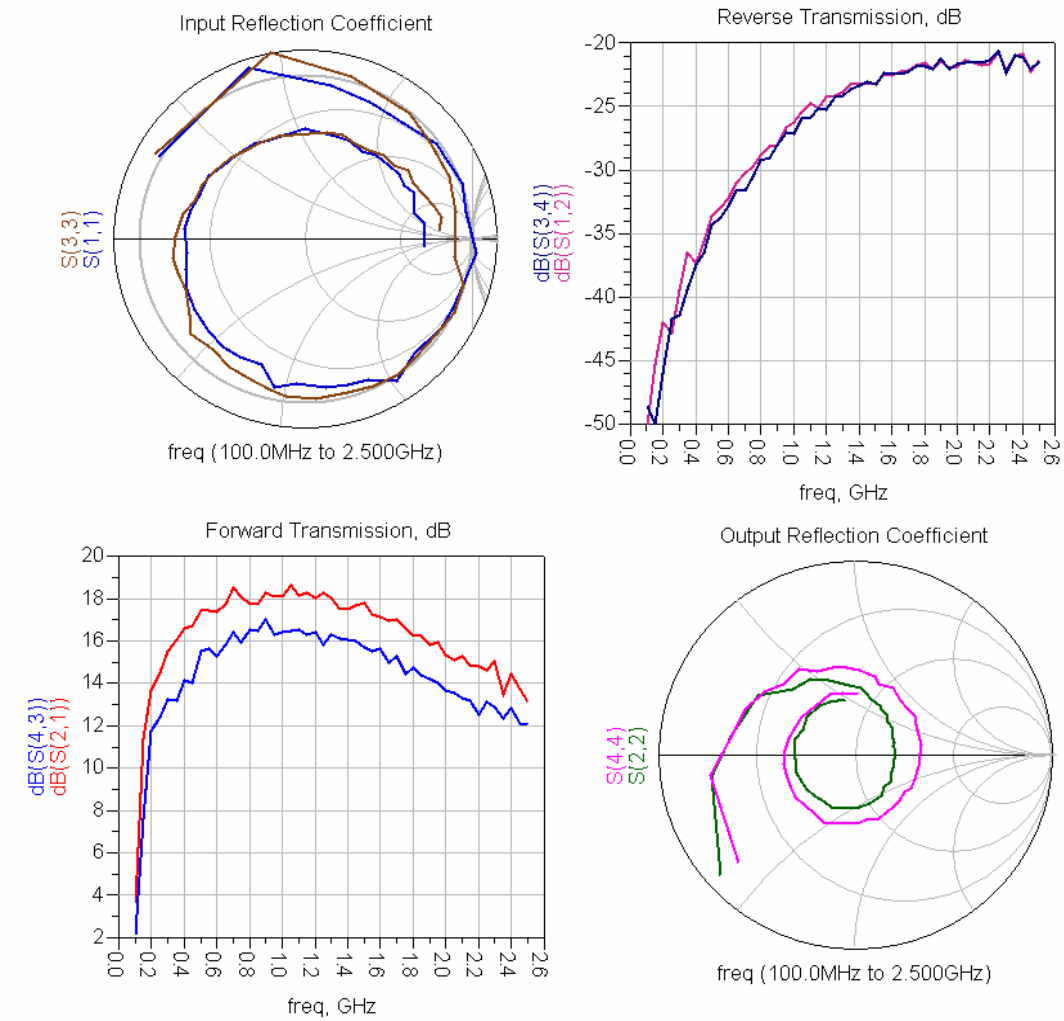

Figure 55: Standard 4 port S parameters measurements for the out-sourced OMMIC test board.

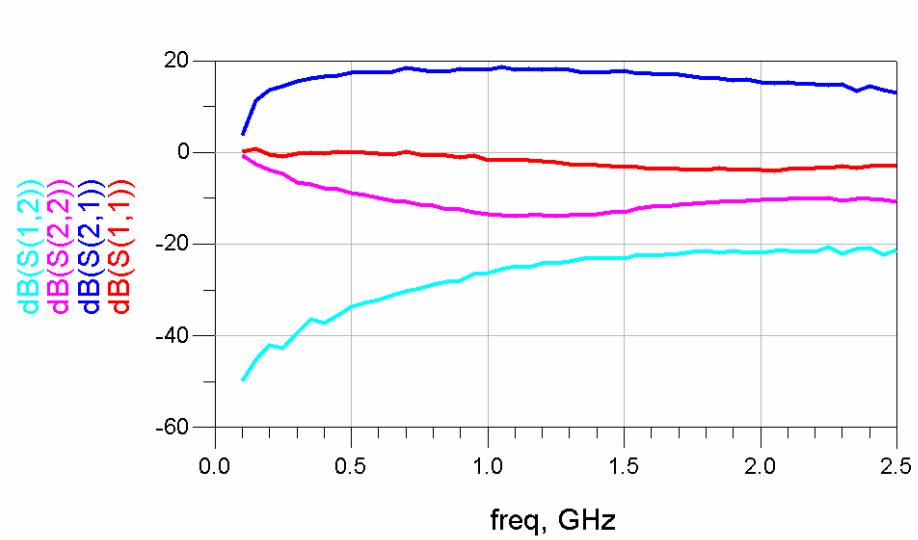

Figure 56: Standard 4-port S-parameters (within required frequency range).

Figure 57 shows the differential s-parameters, also know as mixed-mode s-parameters. These parameters are calculated applying a matrix to the standard 4-port s-parameters. For more information about this parameters see [3].

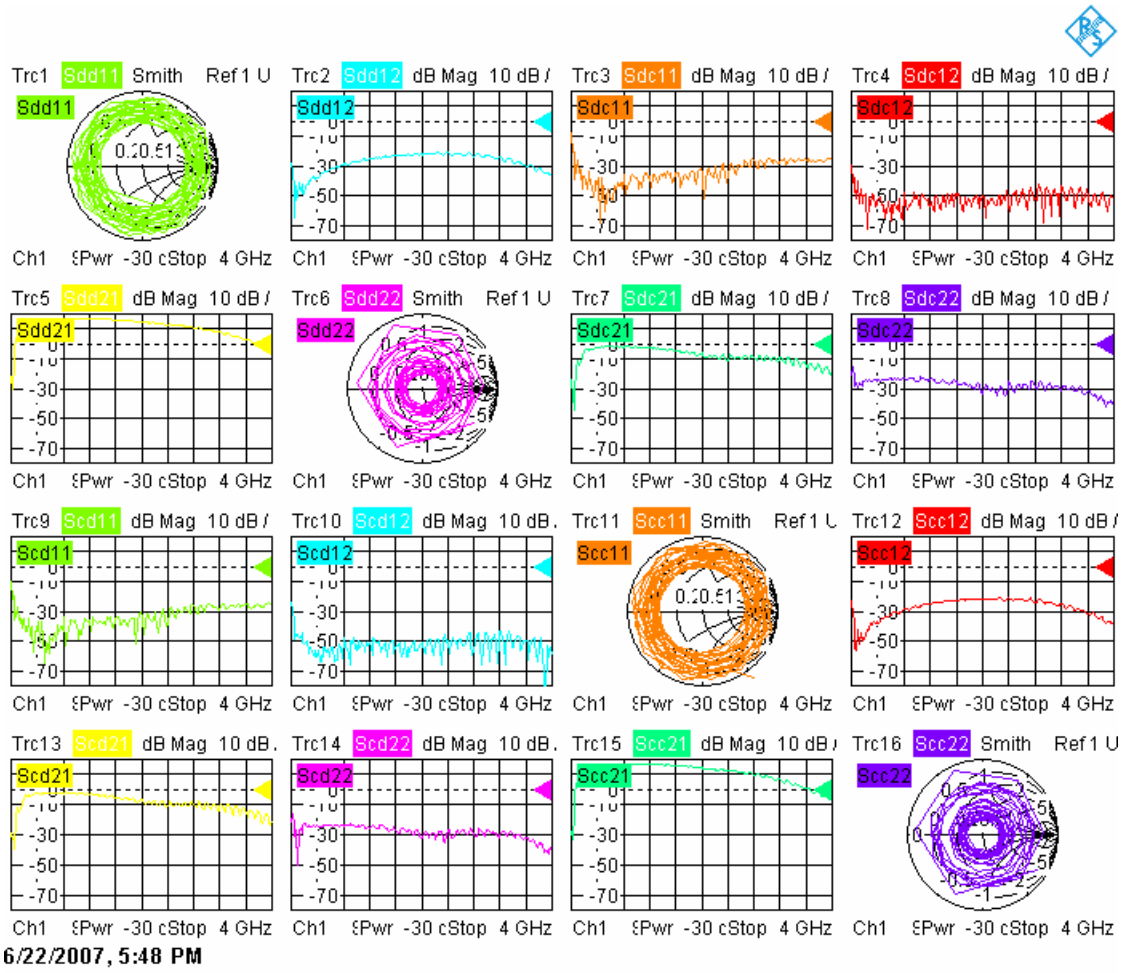

Figure 57: Differential S-parameters for the in-house CGY2109 evaluation board.

3.1.2.– DIFFERENTIAL MEASUREMENTS

The out-sourced evaluation board is not properly designed for differential noise hot-cold measurements. As figure 48 shows there is a coaxial connector in each port, and the amplifier is fully differential. Therefore, differential measurements were carried out using only the in-house test-board.

Figure 47, shows the test-board used in the following measurements. It has an extension that can be modify in order to tune the input noise matching. The shortest and longest line lengths were tried. The set-up for these measurements was described in subsection 2.2.1.2.

Figures 58 and 59 show the noise figure measured for different length differential loads. There is a high peak near 2 GHz that is a mismatch issue between the load and the input stage of the DLNA. Fortunately, this resonance is out of the required frequency band (from 300 MHz to 1GHz)

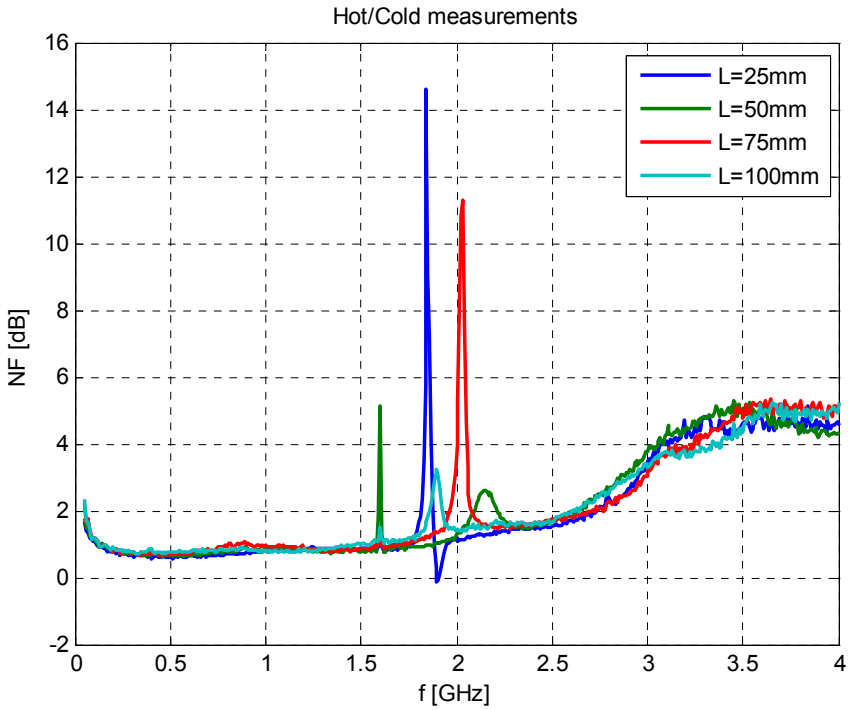

Figure 58: Noise figure (H/C measurements) for different length differential loads.

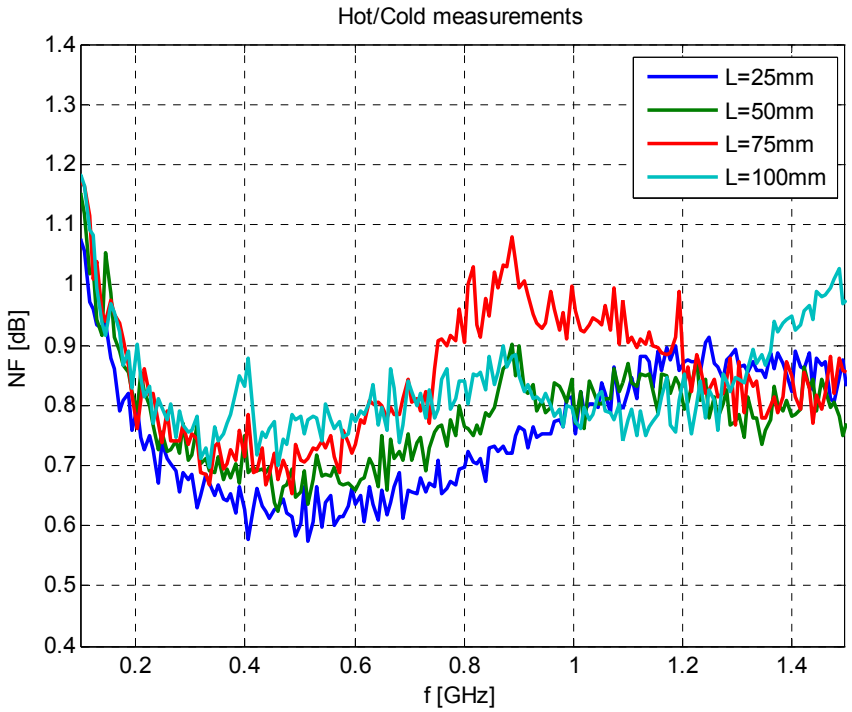

Figure 59: Noise figure (H/C measurements, zoom) for different length differential loads.

Best results were achieved using the shortest differential load (25 mm). Figures 60 and 61 show the noise figure for that differential load. The noise figure varies between 0.6 and 0.8 dB. This curve has a hump around 1.2 GHz that will be tried to be removed in the future.

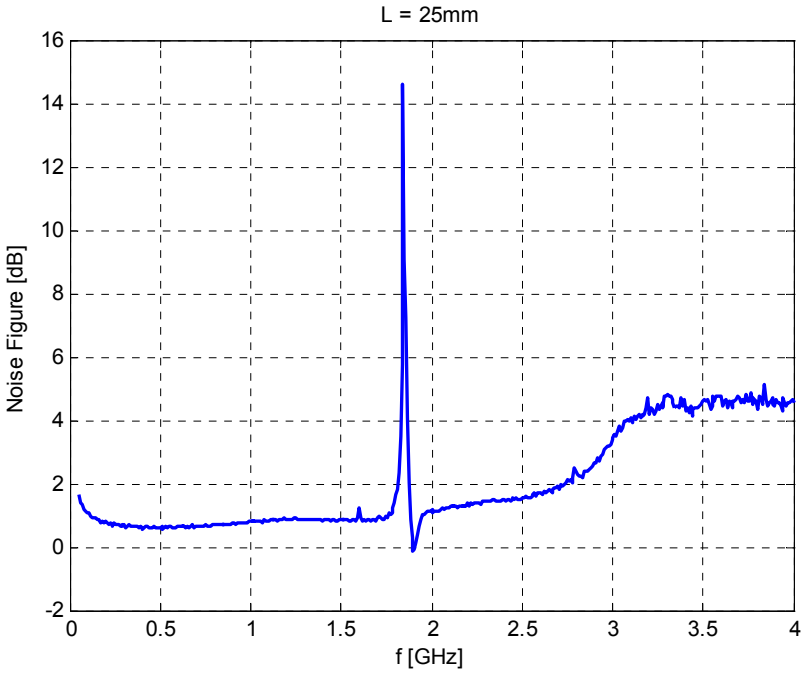

Figure 60: Noise figure (H/C measurements) using a 25 mm load.

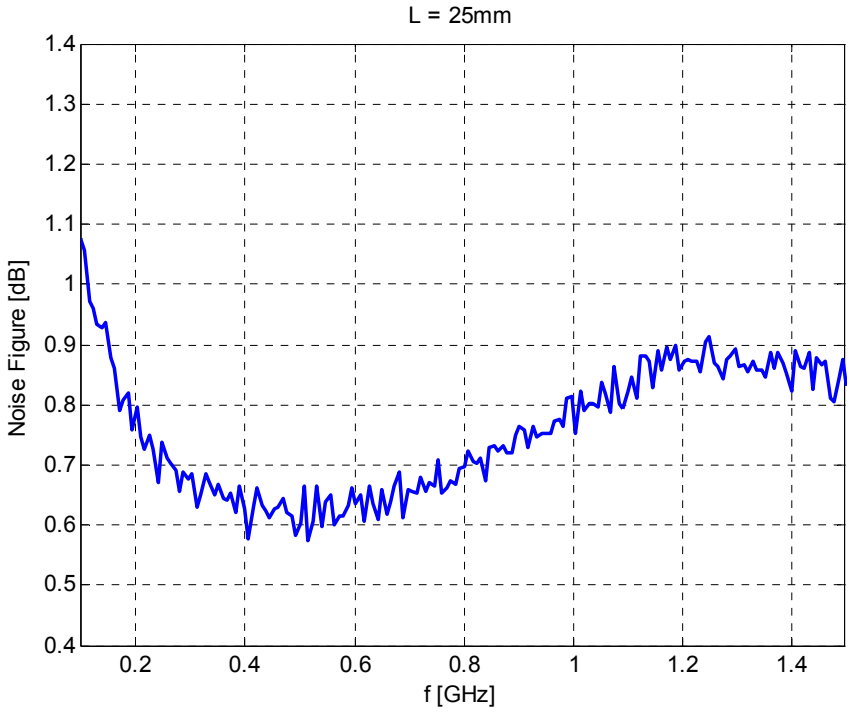

Figure 61: Noise figure (H/C measurements, zoom) using a 25 mm load.

3.2.- CDQ0303-OS (MIMIX)

As in the case of the OMMIC chip, two evaluation boards were tested. One was built in-house and the other was out-sourced (built by MIMIX).

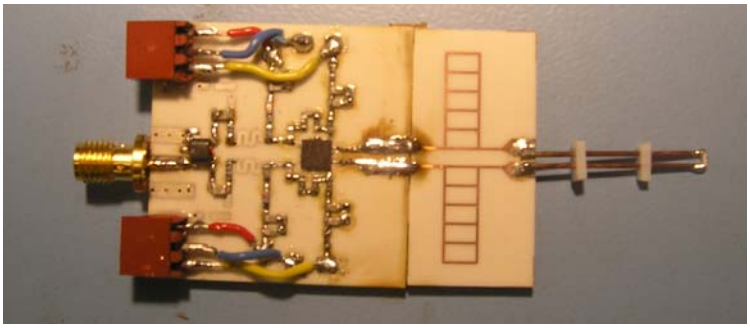

Figure 62: In-house MIMIX test board.

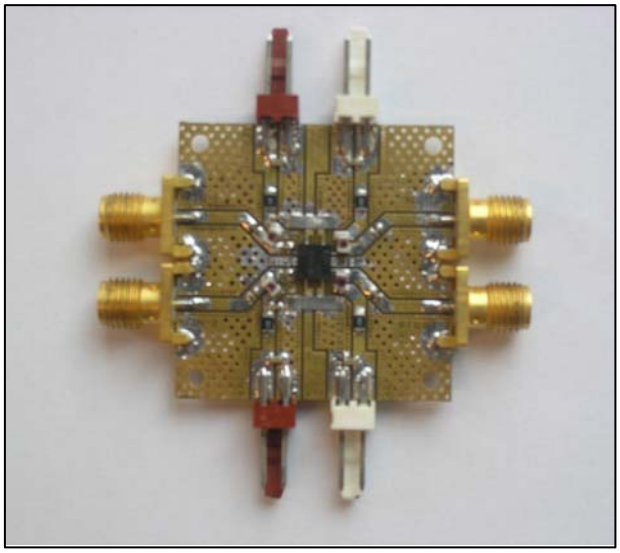

Figure 63: Out-sourced MIMIX test board.

3.2.1.– SINGLE ENDED MEASUREMENTS

3.2.1.1. – IN-HOUSE OMMIC EVALUATION BOARD

MIMIX chip was tested in the same type of evaluation board used for OMMIC ones. The results were not satisfactory (gain too low and noise too high), as figures 64 and 65 show:

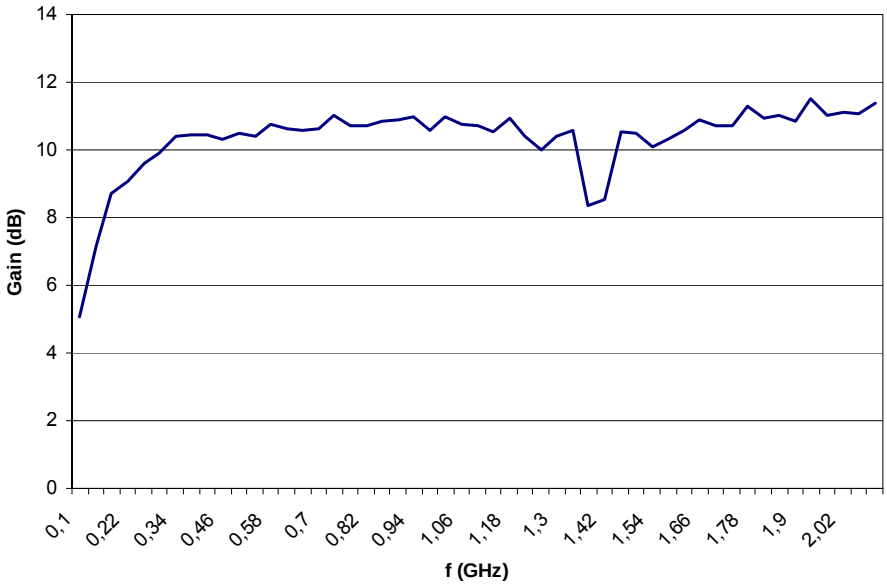

Figure 64: Gain for the in-house MIMIX test board.

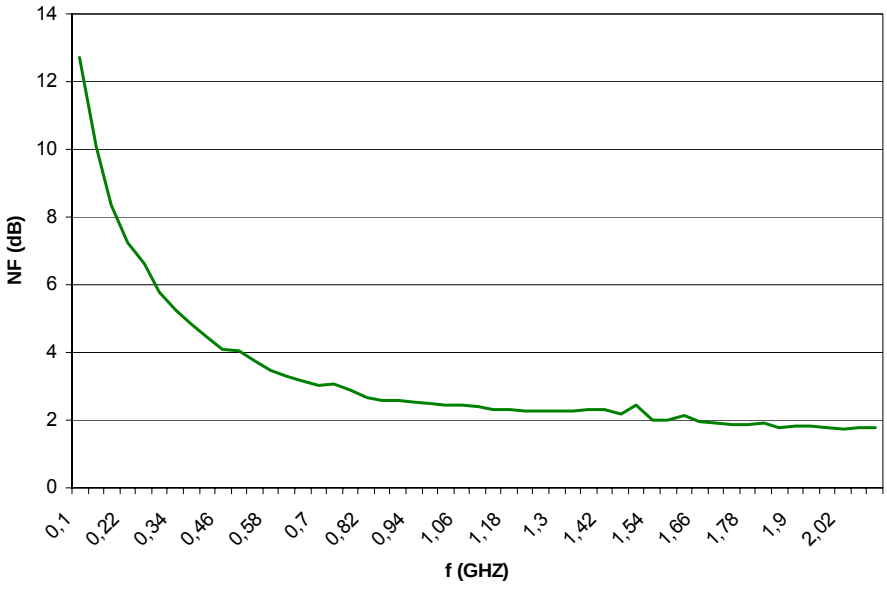

Figure 65: Noise figure for the in-house MIMIX test board.

Both channels were checked for different bias points (the best results are plot above) and without feedback network too. Hot/Cold measurements were postponed to have first good single-ended results.

3.2.1.2. – OUT-SOURCED OMMIC EVALUATION BOARD

The evaluation board provided by MIMIX was tested. Figure 66 and 67 (from noise figure meter N8975A) show the performance of the DLNA, using the following bias points:

- BIAS 1:
  - Vg = -0.4 V
  - Vd = 3 V
  - Id = 43 mA per channel
- BIAS 2:
  - Vg = -0.5 V
  - Vd = 3 V
  - Id = 34 mA per channel

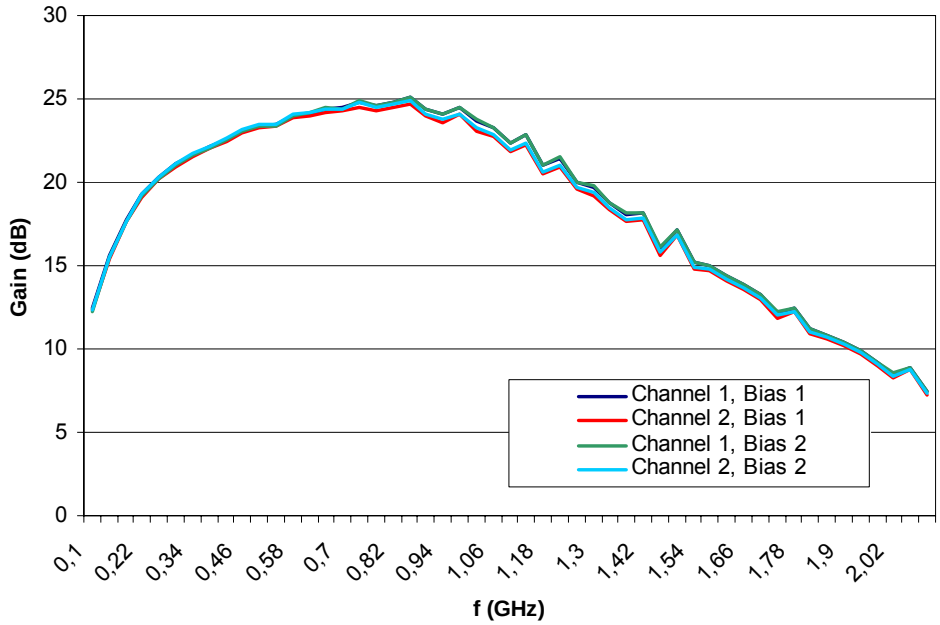

Figure 66: Gain for the out-sourced MIMIX test board.

It is observed that the gain curve has a maximum around 900MHz. In fact, the evaluation board is optimized for an application at 900MHz (see the datasheets [5]). Also there is a perfect matching between the two channels of the balanced DLNA.

The noise figure is in the range of 0.65 dB near 900 MHz and it is so flat from 300 MHz to 1.2 GHz. A spike appears again near 200 MHz in the noise curve.

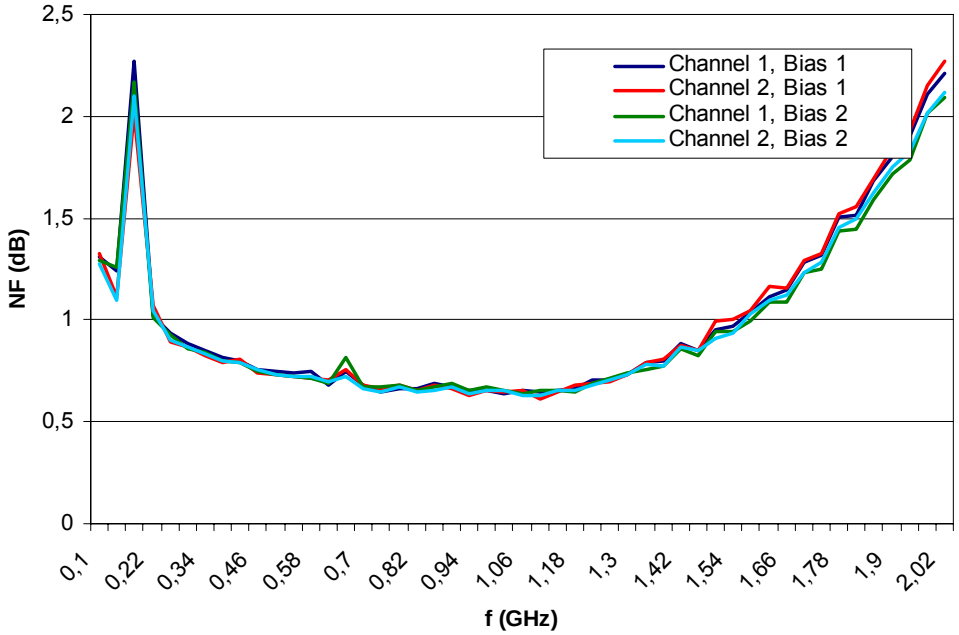

Figure 67: Noise Figure for the out-sourced MIMIX test board.

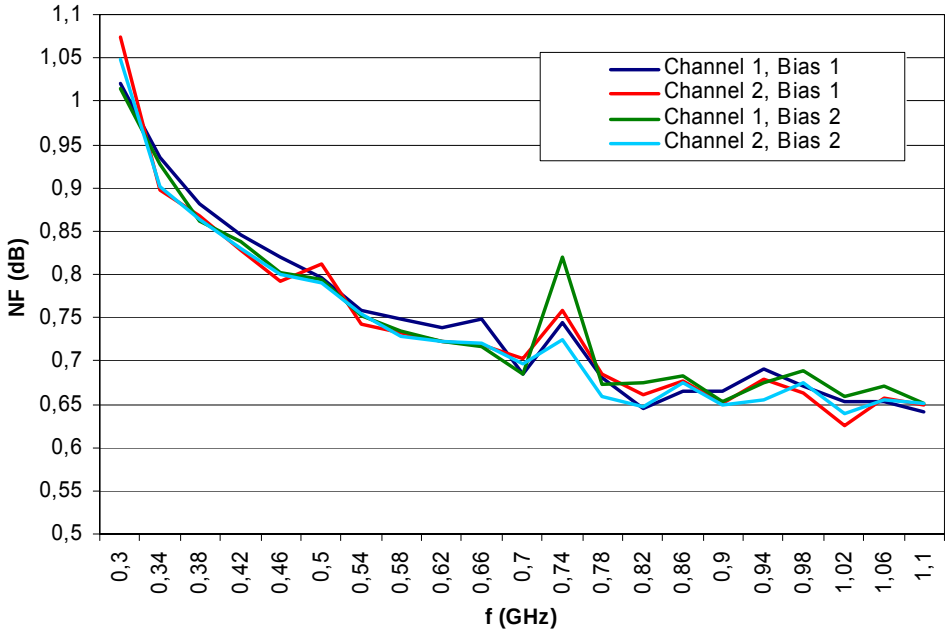

Figure 68: Noise Figure for the out-sourced MIMIX test board (zoom).

The four port s-parameters of the MIMIX evaluation board are shown in figures 69 and 70. The gain is around 20 dB and the input reflection coefficient is also poor (although a bit better compared to the OMMIC test board).

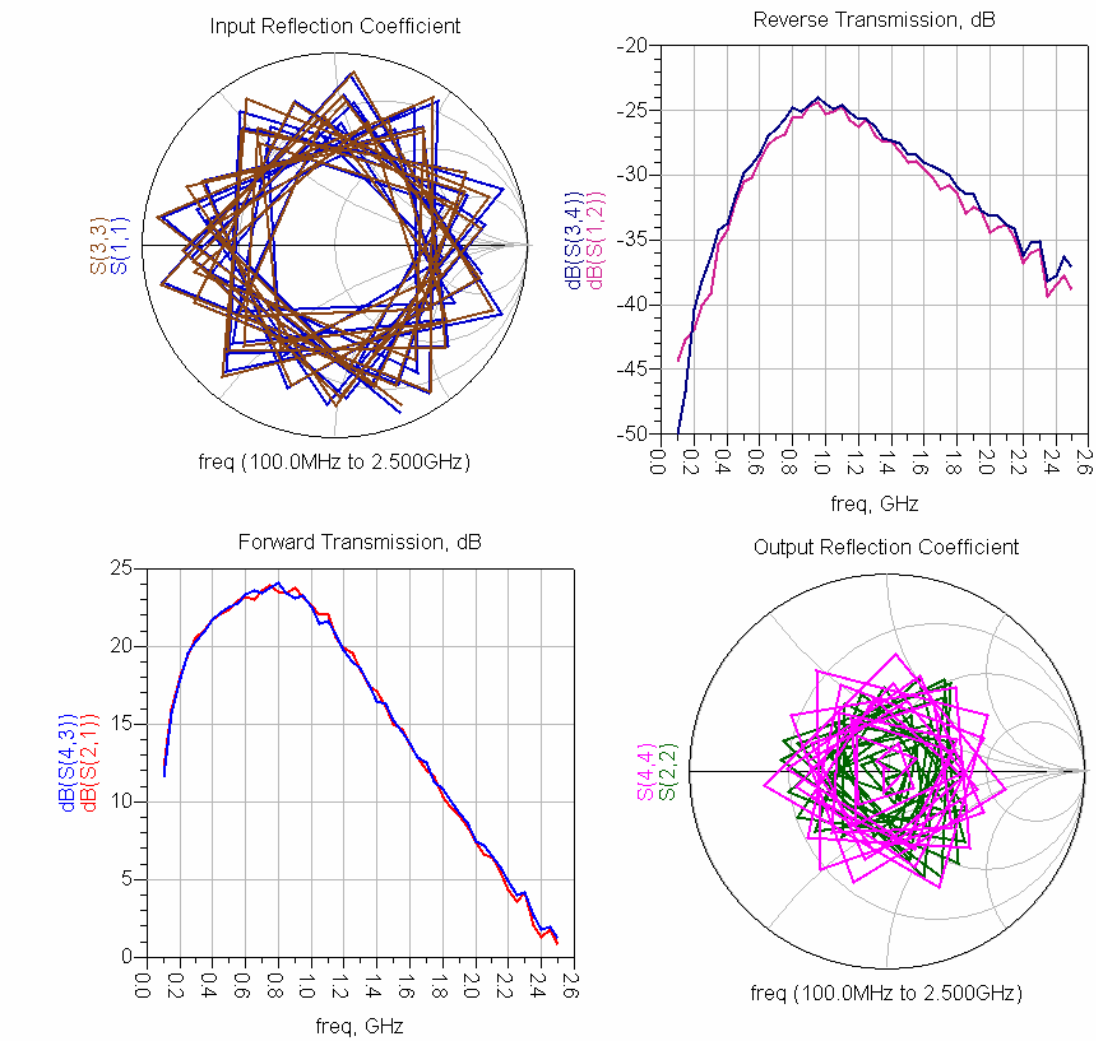

Figure 69: Standard 4 port S parameters measurements for the out-sourced MIMIX test board.

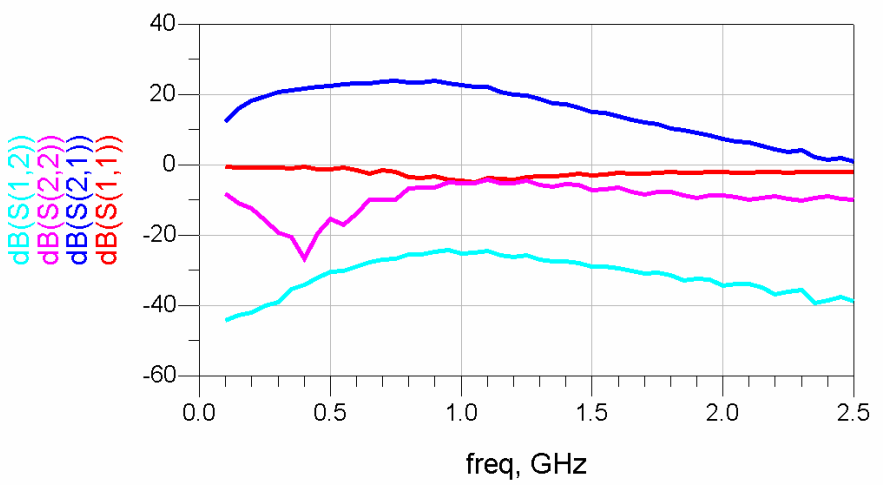

Figure 70: Standard 4-port S-parameters (within required frequency range).

3.2.2.– DIFFERENTIAL MEASUREMENTS

Hot/Cold measurements for the MIMIX DLNA had not been carried out when this report was written. In fact, good results had not been achieved for the MIMIX DLNA using the same in-house evaluation than the OMMIC one.

Therefore, another evaluation board will be designed for the MIMIX amplifier in order to improve the single-ended performance.

3.3.- CGY2109HV vs. CDQ0303-OS

Table 6 summarizes the results of the measurement of the out-sourced test-boards. Notice that the results are quite similar. The gain average is 20 dB and the minimum noise figure achieved is 0,5 dB for OMMIC DLNA and 0,6 dB for the MIMIX one.

	CGY2109HV (OMMIC)	CDQ0303-0S (MIMIX)
300 MHz	G = 18,63 dB	G = 21,09 dB
	NF = 1,06 dB	NF = 1,05 dB
750 MHz	G = 21,079 dB	G = 24,80 dB
	NF = 0,87 dB	NF = 0,72 dB
1 GHz	G = 21,20dB	G = 23,26 dB
	NF = 0,52 dB	NF = 0,64 dB

Table 6: CGY2109HV vs. CDQ0303-OS measurement results.

4.- CONCLUSIONS

COTS differential low noise amplifiers, for integrating within a fully differential active antenna, have been studied. This work is part of the demonstrator FLOWPAD^3 (funded by ASTRON). FLOWPAD^3 is a demonstrator used to show innovative technologies in which low-cost is the main target.

Only the DLNAs CGY2109HV (from OMMIC) and CDQ0303-OS (from MIMIX) fulfil the noise requirements for the mid-band frequency range of the SKA telescope (from 300 MHz to 1 GHz).

Both amplifiers have been evaluated by testing in-house (designed at ASTRON) and out-sourced (provided by the manufacturer) test-boards. Both single-ended and differential measurements were carried out. The gain of both DLNAs was in the range of 20 dB and the noise figure was close to 0.5 dB (35 K of noise temperature) within the required bandwidth. This means that these DLNAs have the potential to reach the noise figure requirements for the SKADS telescopes.

The Hot/Cold Method was extended in order to measure the noise figure for differential amplifiers. This method requires a differential noise source. For this purpose, differential

loads were designed, built and tested. Noise figures close to 0.6 dB were measured using this method.

5.- FUTURE WORK

Attempts will be made to remove the hump in the high frequency part of the required band that appears in the hot-cold measurements results for CGY2109HV (see figure 61).

Also a new in-house evaluation board for the MIMIX DLNA (CDQ0303-OS) will be designed and built in order to carry out hot-cold measurements using differential loads.

6.- REFERENCES

[1] "Memo 69: Reference design for the SKA" International SKA Project Office. Available in: http://www.skatelescope.org/PDF/memos/69_ISPO.pdf

[2] E. de Lera Acedo. "PACMAN FLOWPAD^3 Demonstrator. Antenna Design and Performance Analysis". SKADS DS4T4 report. 2007

[3] W.R. Eisenstadt et al. "Microwave Differential Circuit Design using Mixed-Mode S-parameters". Artech House, 2006.

[4] CGY2109HV/C1. Dual Ultra Low Noise Amplifier with high IP3 0.1 GHz to 3.0 GHz. (Product Brief), OMMIC; Nov. 2006

[5] CDQ0202-OS. 500-600 MHz, Dual, Ultra Low Noise, High IP3 Amplifier. (Product Brief), Mimix Broadband, May 2006.

[6] A. A. Abidi and J. C. Leete. "De-Embedding the Noise Figure of Differential Amplifiers". IEEE Journal of Solid-State Circuits. vol.34, no. 6, June 1999.

[7] J. Morawietz, R.H. Witvers, J. G. Bij de Vaate and E. E. M. Woestenburg. "Noise Characterization of Ultra Low Noise Differential Amplifiers for Next Generation Radiotelescopes". Proceedings of the 37th European Microwave Conference, pp 1570- 1573. October 2007.

[8] J. Morawietz. Internal Report. ASTRON

[9] D.M. Pozar. "Microwave Engineering". 2nd edition John Wiley & Sons,1998. pp 60-62

7.- ACKNOWLEGEMENTS

This work has been supported by the following institutions:

- FG-IGN (Fundación General – Instituto Geográfico Nacional):
  - www.ign.es
  - www.oan.es
- ASTRON (Netherlands Foundation for Research in Astronomy):
  - www.astron.nl
- SKADS (Square Kilometre Array Design Studies):
  - www.skads-eu.org
- Radionet (Advanced Radio Astronomy in Europe)
  - http://www.radionet-eu.org/
- MCCT (Marie Curie Conferences and Training Courses on SKADS):
  - http://mcct.skads-eu.org/